ACS Infectious Diseases

pubs.acs.org/journal/aidcbc

Article

Preclinical Gold Complexes as Oral Drug Candidates to Treat Leishmaniasis Are Potent Trypanothione Reductase Inhibitors

Luiza G. Tunes, Roberta E. Morato, Adriana Garcia, Vinicius Schmitz, Mario Steindel, José D. Corrêa-Junior, Hélio F. Dos Santos, Frédéric Frézard, Mauro V. de Almeida, Heveline Silva, Nilmar S. Moretti, André L. B. de Barros, and Rubens L. do Monte-Neto*

Cite This: https://dx.doi.org/10.1021/acsinfecdis.9b00505

Read Online

ACCESS | Metrics & More | Article Recommendations | Supporting Information

Downloaded via UNIV OF SAO PAULO on April 27, 2020 at 20:59:11 (UTC).
See https://pubs.acs.org/sharingguidelines for options on how to legitimately share published articles.

ABSTRACT: The drugs currently used to treat leishmaniases have limitations concerning cost, efficacy, and safety, making the search for new therapeutic approaches urgent. We found that the gold(I)-derived complexes were active against *L. infantum* and *L. braziliensis* intracellular amastigotes with IC_{50} values ranging from 0.5 to 5.5 μM. All gold(I) complexes were potent inhibitors of trypanothione reductase (TR), with enzyme IC_{50} values ranging from 1 to 7.8 μM. Triethylphosphine-derived complexes enhanced reactive oxygen species (ROS) production and decreased mitochondrial respiration after 2 h of exposure, indicating that gold(I) complexes cause oxidative stress by direct ROS production, by causing mitochondrial damage or by impairing TR activity and thus accumulating ROS. There was no cross-resistance to antimony; in fact, SbR (antimony-resistant mutants) strains were hypersensitive to some of the complexes. BALB/c mice infected with luciferase-expressing *L. braziliensis* or *L. amazonensis* and treated orally with 12.5 mg/kg/day of AdT Et (**3**) or AdO Et (**4**) presented reduced lesion size and parasite burden, as revealed by bioimaging. The combination of (**3**) and miltefosine allowed for a 50% reduction in miltefosine treatment time. Complexes **3** and **4** presented favorable pharmacokinetic and toxicity profiles that encourage further drug development studies. Gold(I) complexes are promising antileishmanial agents, with a potential for therapeutic use, including in leishmaniasis caused by antimony-resistant parasites.

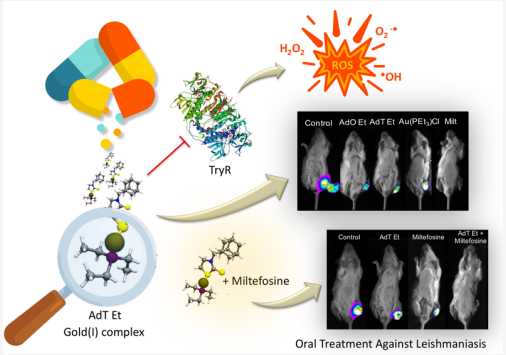

KEYWORDS: *gold(I) complexes, leishmaniasis, antileishmanial, metallodrugs, TR inhibition, oral treatment*

Leishmaniases are a spectrum of diseases caused by *Leishmania* protozoan parasites that are transmitted to mammals through the bite of a female sandfly. These disases are prevalent in 98 countries and are the second-largest parasitic killer after malaria.[1] There are three main forms of leishmaniasis: visceral, cutaneous, and mucocutaneous; this variation depends on the *Leishmania* species involved in the infection and the host immune response. In Brazil, *L. braziliensis* and *L. amazonensis* are the main etiological agents of mucocutaneous and diffuse leishmaniasis, the most severe forms of the cutaneous disease.[2,3]

In the absence of an effective human vaccine against leishmaniasis, their control relies mainly on chemotherapy. The drugs currently used to treat leishmaniasis are pentavalent antimonials (Sb^V), amphotericin B, miltefosine, paromomycin, and pentamidine. The major drawbacks of this limited therapeutic arsenal are toxicity, low efficacy, and the emergence of drug-resistant *Leishmania* parasites.[4] Thus, it is urgent to provide alternative therapeutic strategies against leishmaniasis through the development of new antileishmanial molecules, repurposing of existing drugs, and the creation of new combination schemes.[5]

Gold-based compounds are thiophilic agents recognized by their anti-inflammatory properties that were demonstrated to be promising anticancer and antiparasitic agents.[6−8] Several recent papers demonstrate how prolific the study of anticancer activity of novel gold complexes is.[9−12] There are many proposed mechanisms of action for anticancer gold complexes. The primary target described is thioredoxin reductase: an antioxidant system enzyme, essential to maintain the intracellular redox homeostasis.[13] The antileishmanial activity of gold compounds is still not largely explored. Studies investigating the antileishmanial property of mononuclear cationic or neutral gold(I) complexes containing quinoline functionalized *N*-heterocyclic carbene(s) identified two lead compounds.[14,15] Other studies described a gold(I) inhibitor of

Received: December 18, 2019
Published: April 13, 2020

© XXXX American Chemical Society

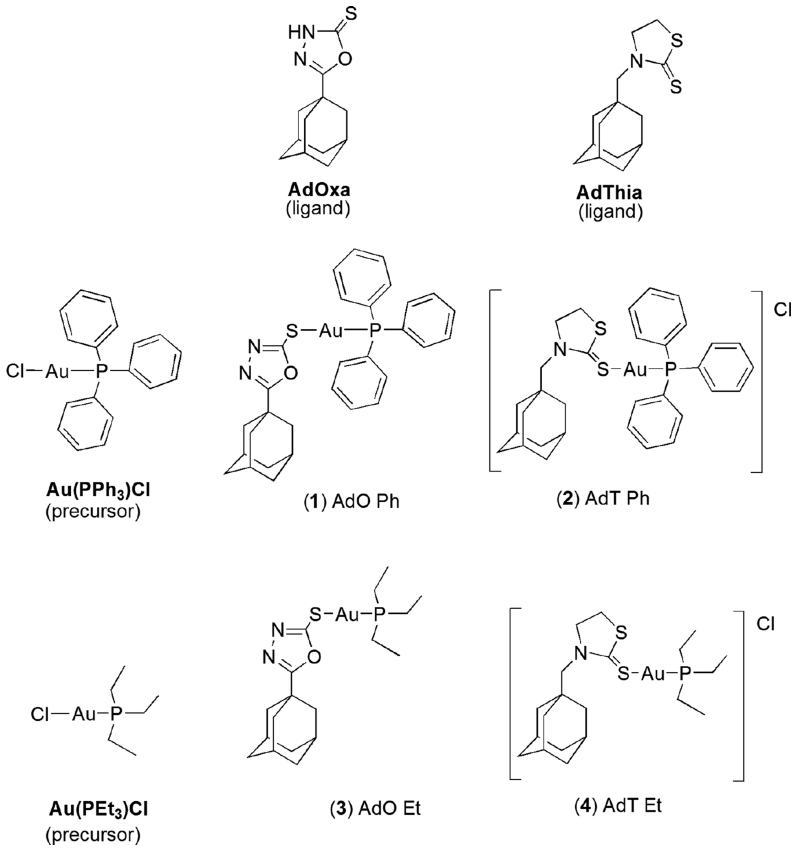

Figure 1. Molecular structures of gold(I) complexes and their respective ligands and precursors.

Table 1. Antileishmanial Activity of Gold(I) Derivatives against *Leishmania* Promastigote and Intracellular Amastigote Forms[a]

	CC_{50} (μM) (95% CI)	IC_{50} (μM) (95% CI) promastigotes		IC_{50} (μM) (95% CI) amastigotes		SI amast. THP-1	
compound	THP-1 MΦ	*L. infantum*	*L. braziliensis*	*L. infantum*	*L. braziliensis*	*Li*	*Lb*
AdThia ligand	>100	>100	>100	ND	ND	ND	ND
AdOxa ligand	18.51 (17.13–2)	>100	>100	ND	ND	ND	ND
AdO Ph (**1**)	5.33 (4.51–6.31)	5.95 (5.47–6.47)	6.34 (3.26–12.33)	1.58 (1.21–2)	5.56 (4.83–6.7)	3.37	0.95
AdT Ph (**2**)	5.60 (4.72–6.65)	3.19 (2.73–3.73)	5.09 (4.40–5.89)	1.03 (0.68–1.5)	2.29 (1.9–2.77)	4.05	2.44
AdO Et (**3**)	3.08 (2.76–3.44)	1.48 (1.37–1.60)	1.70 (1.58–1.83)	0.54 (0.45–0.6)	2.35 (2.13–2.58)	5.7	1.31
AdT Et (**4**)	4.08 (3.69–4.50)	0.95 (0.8–1.11)	1.92 (1.78–2.08)	1.09 (0.96–1.2)	2.8 (2.53–3.1)	3.73	1.45
$Au(PPh_3)Cl$[b]	4.98 (4.64–5.33)	4.53 (3.91–5.26)[36]	5.25 (4.65–5.93)	0.9 (0.58–1.36)	2.83 (2.57–3.12)	5.53	1.75
$Au(PEt_3)Cl$[b]	5.43 (5.08–5.79)	1.94 (1.61–2.33)[36]	2.79 (2.51–3.10)	1.35 (1.15–1.6)	3.31 (2.79–3.93)	3.77	1.64
amphotericin B[b]	12 (11.43–12.59)	0.1 (0.01–0.11)	0.1 (0.09–0.11)	0.09 (0.08–0.09)	0.12 (0.10–0.15)	133.33	100
miltefosine[b]	39.08 (37.6–40)	ND	ND	0.57 (0.54–0.6)	6.68 (5.55–8.03)	68.56	5.85

[a]Selectivity indexes are shown on the basis of the cytotoxic activity performed on human THP-1 macrophages. CC_{50}: cytotoxic concentration to 50% of THP-1 host macrophages; IC_{50}: inhibitory growth concentration to 50% of the parasites; ND: not determined; 95% CI: 95% confidence interval; AdThia: adamantane thiazolidine; AdOxa: adamantane oxadiazole; SI: selective index calculated by CC_{50} THP-1/IC_{50} amast. [b]$Au(PPh_3)Cl$ and $Au(PEt_3)Cl$: the data concerning antileishmanial controls and gold(I) precursors were previously published by Chaves et al.[19] Statistical comparisons of selected Table 1 data are presented in Figure 2. The data are the mean of at least two independent experiments performed in triplicate. Original sensitivity profiling curves are presented in Figure S1.

NADH fumarate reductase,[16] a gold(III) DNA interacting agent,[17] and four gold(I) and -(III) derivatives that are potent inhibitors of *L. mexicana* cysteine protease CPB2.8ΔCTE.[18] Our group has recently described ten novel antileishmanial gold(I) complexes containing phosphine and 5-phenyl-1,3,4-oxadiazole-2-thione.[19]

Recent studies revealed that auranofin (Ridaura), a gold(I) triethylphosphine thiosugar drug used to treat rheumatoid arthritis, exerts anticancer and antiparasitic activities primarily by targeting thioredoxin reductase and thioredoxin-glutathione reductase redox systems.[20−25] Auranofin was shown to exhibit *in vitro* and *in vivo* antileishmanial activity with the ability to inhibit trypanothione reductase (TR), a crucial enzyme for redox homeostasis in trypanosomatid protozoa including *Leishmania*.[26,27] The auranofin-mediated redox homeostasis disruption in *Leishmania* involves TR inhibition through two mechanisms: the gold center of auranofin binds to cysteine residues present at the active site of the enzyme, and the thiosugar part of the molecule binds to the trypanothione binding site.[27] Inspired by the promising antileishmanial

https://dx.doi.org/10.1021/acsinfecdis.9b00505
ACS Infect. Dis. XXXX, XXX, XXX−XXX

properties of auranofin, we decided to investigate new gold(I)-derived compounds as metallodrugs against leishmaniasis.

Aiming to develop gold(I) TR inhibitors with encouraging pharmacological properties and antileishmanial activity, we investigated gold(I) triphenylphosphine- and triethylphosphine-based complexes with thioadamantane ligands, since they inhibit thioredoxin reductase (TrxR) enzyme from mammalian cells.[28] We studied the *in vitro* antileishmanial activity and mode of action as well as their *in vivo* oral efficacy and combination with miltefosine. The findings reported here show that gold(I) complexes could be promising antileishmanial drug candidates and chrysotherapy deserves to be further investigated as an alternative for leishmaniasis treatment.

RESULTS

When complexed with $Au(PPh_3)Cl$, the binding of the adamantane ligand to oxadiazole or thiazolidine (AdOxa and AdThia, Figure 1) forms the compounds triphenylphosphine-[5-adamantyl-1,3,4-oxadiazole-2-thiolate(κS)]gold(I), AdO Ph (**1**), and triphenylphosphine[(methyl-1-adamantane)1,3-thiazolidine-2-thione(κS)]gold(I), AdT Ph (**2**), respectively. Similar reactions performed using the precursor $Au(PEt_3)Cl$ yields compounds triethyllphosphine[5-adamantyl-1,3,4-oxadiazole-2-thiolate(κS)]gold(I), AdO Et (**3**), and triethylphosphine[(methyl-1-adamantane)1,3-thiazolidine-2-thione(κS)]gold(I), AdT Et (**4**) (Figure 1).

Gold(I) Complexes Exert Potent *In Vitro* Antileishmanial Activity. Gold(I) complexes and their precursors were highly active against *L. infantum*, presenting IC_{50} values ranging from 0.9 to 10 μM against promastigotes and from 0.5 to 4 μM against intracellular amastigotes (Table 1). Therefore, they were more selective against the clinically relevant evolutive form of the parasite, the intracellular amastigotes. Gold(I) complexes presented significant toxicity to THP-1 cells, with CC_{50} varying between 4.08 and 5.6 μM and selectivity indexes ranging from 3.37 to 5.7 μM and 0.95 to 2.44 μM, respectively, for *L. infantum* and *L. braziliensis* (Table 1). The ligands were not active or presented low activity on parasites and were not toxic to THP-1 cells (Table 1). Gold(I) complexes derived from triethylphosphine (complexes **3** and **4**) were more active than those derived from triphenylphosphine (complexes **1** and **2**). To highlight this structure−activity relationship evidence, IC_{50} averages were compared among the groups selected from Table 1 (Figure 2). Indeed, triethylphosphine gold(I) derivatives are more active against *Leishmania* spp. promastigote forms, THP-1 macrophages, and when comparing oxadiazole-substituted compounds against intracellular amastigotes (Figure 2). Thiazolidine-derived AdT Ph (**2**) and AdT Et (**4**) did not differ in activity against *Leishmania* spp. intracellular amastigote forms, suggesting a host-dependent role in thiazolidine-associated pharmacodynamics (Figure 2). In general, *L. infantum* amastigotes were more susceptible to all gold(I) complexes (Figure 2). Drug sensitivity in *L. braziliensis* intracellular amastigotes was reduced (IC_{50} varying from 2.5 to 5.6) when compared to *L. infantum* (IC_{50} ranging between 0.5 and 1.6) (Table 1). As gold(I) complexes **1**−**4** were highly active against both *L. infantum* and *L. braziliensis*, they were selected for further experiments to investigate their antileishmanial potential and mode of action. Gold(I) complexes were more active against *L. braziliensis* intracellular amastigotes than the reference compound miltefosine (Table 1). Complex AdO Et (**3**) presented activity against *L. infantum* intracellular amastigotes, which is comparable with miltefosine, respectively, at 0.54 and 0.57 μM (Table 1).

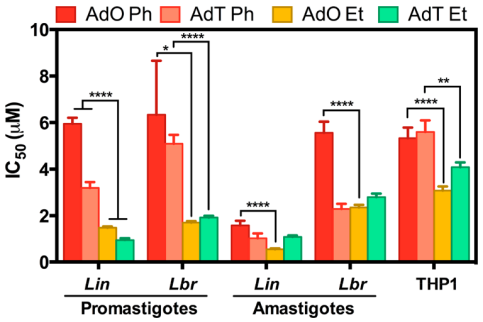

Figure 2. Comparative antileishmanial and cytotoxicity effect of gold(I) triethylphosphine and triphenylphosphine derivatives. Compounds were assayed against promastigote and amastigote forms of *Leishmania infantum* and *Leishmania braziliensis*. Gold(I) complexes were more active against *L. infantum* intracellular amastigotes. Thiazolidine-derived compounds do not differentiate activity between Ph- or Et-substituted groups. The average of IC_{50} values were obtained from Table 1. Students *t*-test: *$p = 0.02$; **$p = 0.006$; ****$p < 0.0001$. *Lin*: *L. infantum*; *Lbr*: *L. braziliensis*; THP1: human monocyte-derived macrophage cell line.

Gold(I) Complexes Inhibit Trypanothione Reductase Activity. Because auranofin is able to inhibit TR,[27,29] one of the proposed mechanisms of action for the gold(I) complexes is TR inhibition. We observed that all tested complexes were able to inhibit the enzyme TR with IC_{50} and IC_{90} values approximately 10-fold more potent than the positive control clomipramine (Table 2). TR inhibitory concentrations correlate with IC_{50} values obtained in an antipromastigote activity assay, supporting the involvement of TR as a putative target for complexes **1**−**4**. Triethylphosphine-derived complexes (**3** and **4**) and their precursor were more active than those based on triphenylphosphine (**1** and **2**), which corroborates data obtained on antipromastigote activities (Table 1). Also, IC_{50} values for complexes **2**, **3**, and **4** are similar to their IC_{90} values, confirming that total TR inhibition can be achieved with a low concentration of these three complexes, a similar pattern that was also observed only for the $Au(PEt_3)Cl$ gold(I) precursor (Table 2). The correlation analysis between gold complex TR inhibition activity and gold complex antipromastigote activity revealed correlation coefficients of 0.9985 ($p = 0.0008$) and 0.8841 ($p = 0.05$), respectively, for *L. infantum* and *L. braziliensis* (Figure S2).

Table 2. Inhibitory Activity of Complexes 1−4 on Trypanothione Reductase Enzyme[a]

	trypanothione reductase inhibition	
compound	IC_{50} (μM) ± SD	IC_{90} (μM) ± SD
1, AdO Ph	7.25 ± 1.28	23.02 ± 1.81
2, AdT Ph	3.63 ± 0.31	4.43 ± 0.33
3, AdO Et	1.74 ± 0.14	2.25 ± 0.18
4, AdT Et	1.08 ± 0.08	2.42 ± 0.12
$Au(PPh_3)Cl$	7.84 ± 1.31	29.65 ± 2.14
$Au(PEt_3)Cl$	1.07 ± 0.51	1.43 ± 0.19
clomipramine	14.58 ± 0.51	108.9 ± 2.14

[a]Clomipramine: positive control;[30] IC_{50} and IC_{90}: compound concentrations that inhibit, respectively, 50% and 90% of enzyme activity.

https://dx.doi.org/10.1021/acsinfecdis.9b00505
ACS Infect. Dis. XXXX, XXX, XXX−XXX

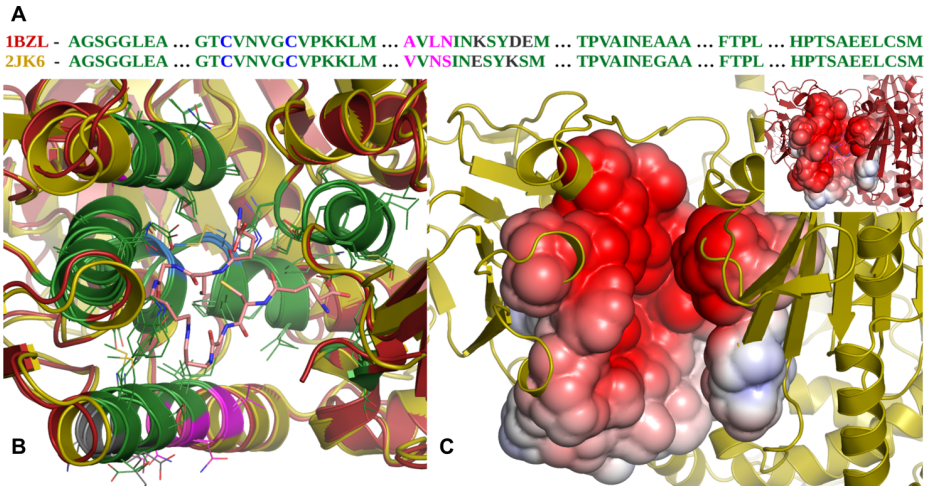

Figure 3. Amino acid sequence alignment of the active sites of *T. cruzi* TR (1BZL) and *L. infantum* TR (2JK6) (A). Alignment of the three-dimensional structure of the active site cavities of *T. cruzi* TR (red) and *L. infantum* TR (olive). Highlighted conserved residues (green), different residues (magenta and gray), catalytic cysteine pairs (blue), and trypanothione (pink). (B). Electrostatic profile of the active site cavity of *L. infantum* TR. (C) Electrostatic profile of *T. cruzi* TR at the top right corner. The electrostatic potential varies from −5 (red) to 5 (blue) kT/e.

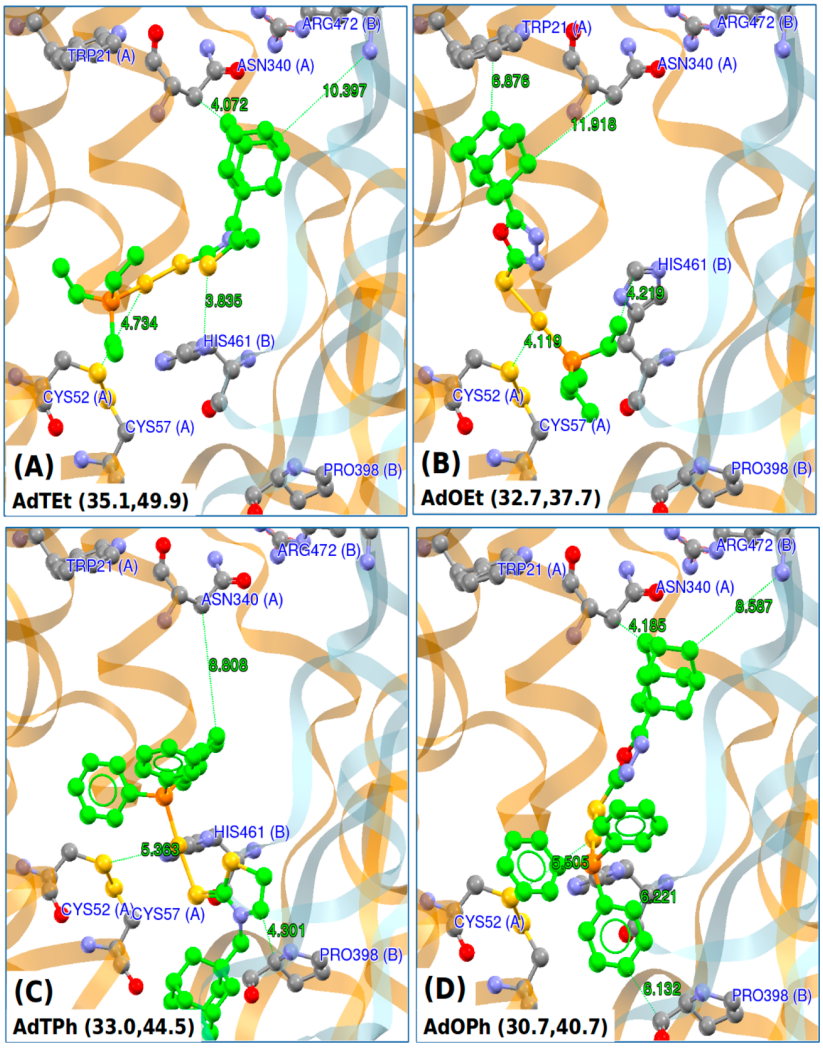

Figure 4. Docking modes predicted for the gold complexes and *Leishmania infantum* TR (PDB code 2JK6). Only the best pose for each ligand is represented. The main protein residues are also highlighted and labeled. The values in parentheses are the average and highest score, respectively.

https://dx.doi.org/10.1021/acsinfecdis.9b00505
ACS Infect. Dis. XXXX, XXX, XXX−XXX

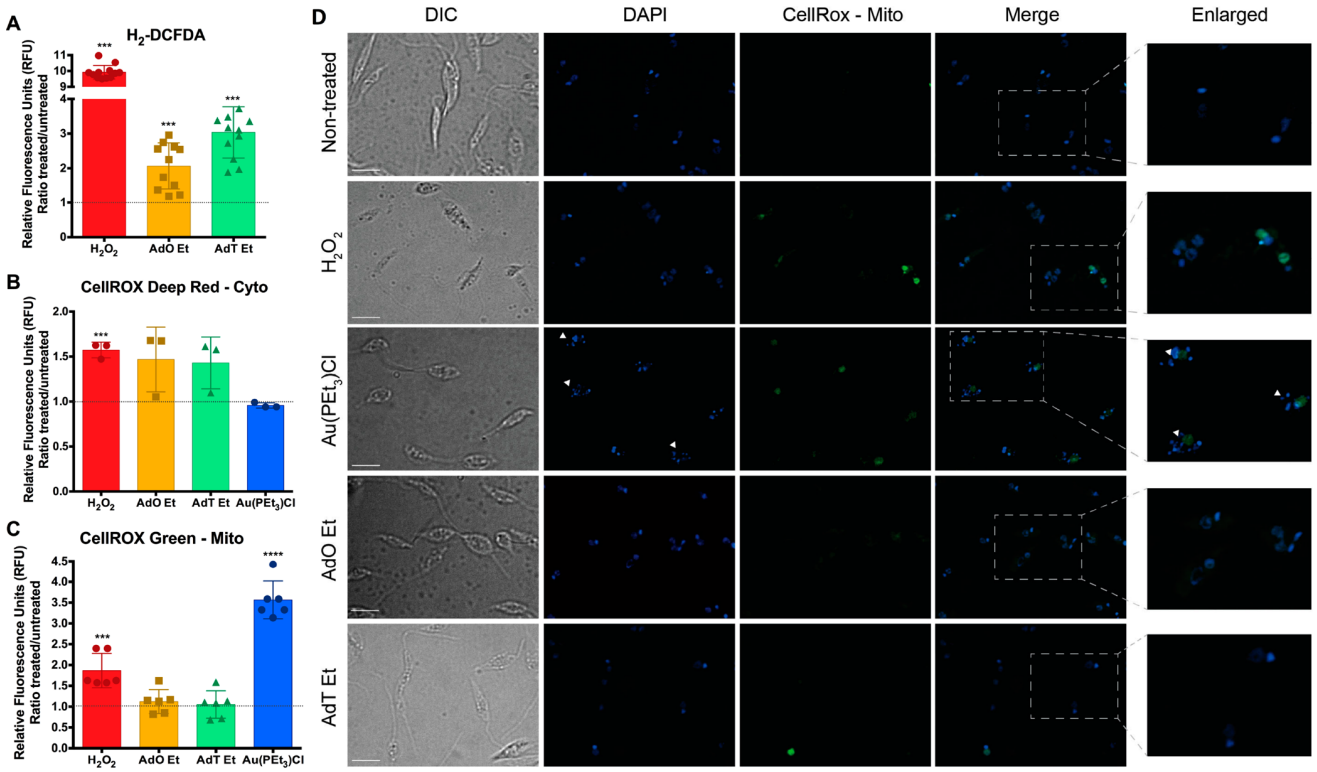

Figure 5. ROS production in *L. braziliensis* after treatment with gold(I) complexes. The treatment of promastigote forms for 2 h with an IC_{50} of gold(I) complexes increases ROS production in the cytoplasm as detected by H_2-DCFDA (A) or CellROX Deep Red reagent (B). An increase in nuclear and mitochondrial ROS production was also observed after treatment with $Au(PEt_3)Cl$ as measured by CellROX Green reagent (C) or by immunofluorescence (D). Extensive DNA damage was observed after $Au(PEt_3)Cl$ as shown by the arrowheads. Scale bar: 10 μm. DIC: differential interference contrast (brightfield). Statistical differences between parasites treated with $Au(PEt_3)Cl$, AdO Et, or AdT Et and the untreated counterpart were calculated using the Student's *t*-test: for H_2-DCFDA, ***p = 0.00002; for CellRox DeepRed, ***p = 0.0004; for CellRox Green, ***p = 0.0004 and ****p < 0.0001.

We understand the limitations for using *T. cruzi*-derived TR instead of *Leishmania* TR, but we had no access to purified or recombinant *Leishmania* TR. Because of that, we performed docking of the gold(I) complexes with *L. infantum* TR as well as performed comparative structural analysis and electrostatic profiling of the two enzymes. *L. infantum* TR is very similar to *T. cruzi* TR, for which the gold complexes demonstrated satisfactory inhibitory indexes. Amino acid sequence alignment of TR from *T. cruzi* (PDB code 1BZL) and *L. infantum* (PDB code 2JK6) shows 90% identity in the residues forming the active site of the enzyme (Figure 3A). Moreover, the residues in the cavity of the active site where the substrate trypanothione docks are formed by identical residues (Figure 3B). Thus, the active site cavity presents the same shape in both enzymes. The electrostatic profiles in the active site for *T. cruzi* TR and *L. infantum* TR (Figure 3C) are also very similar in both enzymes. These observations allowed us to conclude that the binding of substrate in both enzymes should occur in a similar way, assuming the same conformation. The best poses predicted for each ligand and *L. infantum* TR are shown in Figure 4, with the docking search region represented by green dots. Due to the small size of the ligands compared to the binding site and the lack of specific anchor points, distinct poses are predicted with very close scores. Only hydrophobic contacts are observed between the receptor and ligands, and in most cases, the adamantane group is found to be close to Asn340(A) and Arg472(B) residues. The phosphines lie close to the redox-active moiety (Cys52(A)−Cys57(A)) and His461(B), keeping the Au···S distance around the specified bounds (1.5−3.5 Å). For ligands with PEt_3 phosphines the Au···S(Cys52(A)), the distance was 4.1−4.7 Å, and for those with bulky PPh_3, it was 5.1−5.3 Å. Using the average score as a reference, the ligand−receptor affinity is ordered as AdT Et > AdT Ph ∼ AdO Et > AdO Ph, with the complex AdT Et showing the highest absolute score (49.9). The mechanism would include the docking of the ligand with the hydrophobic adamantane group pointed toward the open end of the binding cavity and the phosphine buried close to the Cys52(A) residue (Figure 4A). This arrangement keeps the gold atom ∼4 Å from S(Cys52) and promptly reacts to release the thiazolidine ligand.

Gold(I) Complexes AdO Et and AdT Et Induce Oxidative Stress in *L. braziliensis*. Since AdO Et (**3**) and AdT Et (**4**) were able to inhibit TR at low concentrations and TR is responsible for the detoxification of the reactive oxygen species (ROS), we decided to investigate if they would increase ROS production/accumulation. To test for this, we quantified ROS levels using two different fluorescent probes: H_2-DCFDA and CellROX Deep Red, which detect thiol derivative and superoxide ROS species, respectively. We found a 2- to 3-fold increase for thiol derivative ROS following a 2 h exposure of *L. braziliensis* to the IC_{50} of AdO Et or AdT Et, respectively, and about a 1.5-fold increase in superoxide species for both compounds (Figure 5A,B). To gain insight on the effect of these compounds in ROS production, we also measured nuclear and mitochondrial ROS production after treatment

https://dx.doi.org/10.1021/acsinfecdis.9b00505
ACS Infect. Dis. XXXX, XXX, XXX−XXX

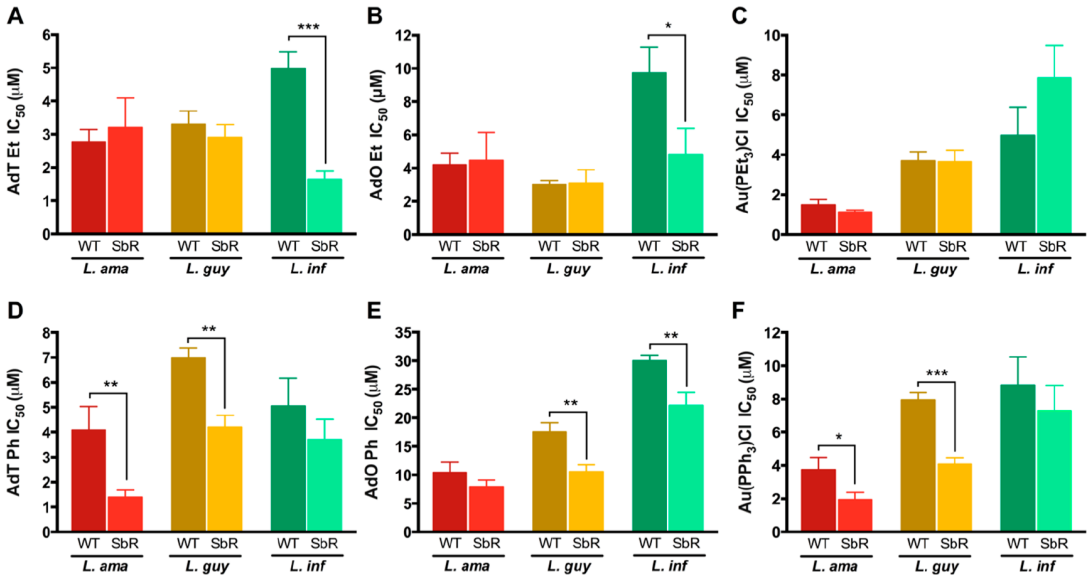

Figure 6. Antileishmanial activity of gold(I) complexes and their precursors against Sb-sensitive and Sb-resistant *Leishmania* spp. parasites. Results shown are the average of at least two independent experiments performed in triplicate. AdT Et (A); AdO Et (B); $Au(PEt_3)Cl$ (C); AdT Ph (D); AdO Ph (E); $Au(PPh_3)Cl$ (F). Statistical differences were calculated using the Student's *t*-test: $*p < 0.05$; $**p < 0.01$; $***p < 0.001$. *L. ama*: *Leishmania amazonensis* (red bars); *L. guy*: *L. guyanensis* (yellow bars); *L. inf*: *L. infantum* (green bars). The dark color (left bars) represents the IC_{50} of gold(I) complexes against WT parasites, while in SbR mutants are shown in the light color (right bars). The data are the mean of at least two independent experiment performed in triplicate

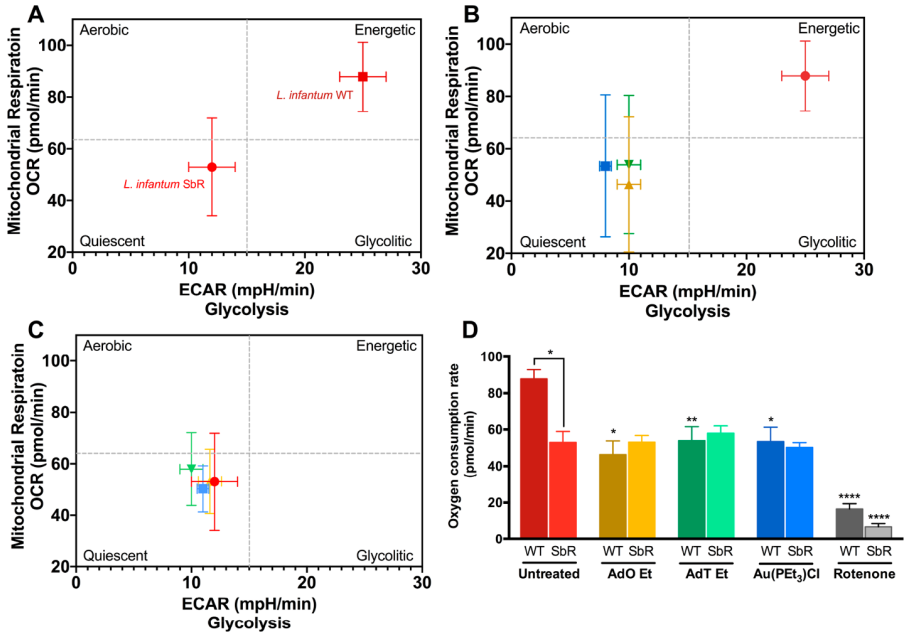

Figure 7. Cell energy phenotype. Mitochondrial respiration (oxygen consumption rate, OCR) versus glycolysis (extracellular acidification rate, ECAR) rates of *L. infantum* WT and SbR parasites (A). Energy phenotype of untreated *L. infantum* WT compared to parasites treated with $Au(PEt_3)Cl$, AdT Et, or AdO Et (B). Energy phenotype of untreated *L. infantum* SbR compared to parasites treated with $Au(PEt_3)Cl$, AdT Et, or AdO Et (C). Oxygen consumption average of gold(I) treated and untreated WT and SbR *L. infantum*. Statistical differences between parasites treated with $Au(PEt_3)Cl$, AdO Et, or AdT Et and the untreated counterpart (WT or SbR) were calculated using the Student's *t*-test: $*p < 0.05$; $**p < 0.01$; $****p < 0.0001$ (D). Results are presented as means of three independent experiments, performed at least in triplicate. *L. infantum* WT (dark red) and SbR (red); AdO Et (yellow); AdT Et (green); $Au(PEt_3)Cl$ (blue). Rotenone is an inhibitor of the mitochondrial respiratory chain complex I.

with AdO Et and AdT Et, using the oxidative stress detection probe CellROX Green. Two hours of exposure with IC_{50} of $Au(PEt_3)Cl$ leads to a 4-fold increase in ROS levels compared to nontreated parasites (Figure 5C); no effect was observed with AdO Et or AdT Et. Finally, using fluorescence microscopy, we confirmed the increase in nuclear and mitochondrial ROS levels (Figure 5D). The exposure of parasites to $Au(PEt_3)Cl$ causes extensive DNA damage, as observed by DAPI staining, compared to nontreated parasites or those exposed to AdO Et or AdT Et (Figure 5D). Thus,

https://dx.doi.org/10.1021/acsinfecdis.9b00505
ACS Infect. Dis. XXXX, XXX, XXX−XXX

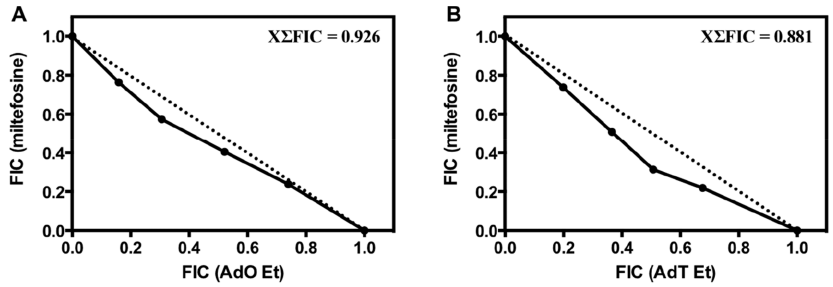

Figure 8. Isobologram representing the *in vitro* interaction between AdO Et and miltefosine (A) and AdT Et and miltefosine (B) against *L. braziliensis* intracellular amastigotes. Assays were performed by a fixed-ratio method based on the IC_{50}'s, in which constant proportions of AdO/miltefosine or AdT/miltefosine concentrations are tested: 100:0; 80:20; 60:40; 20:80; 0:100. Results are presented as means of at least two independent experiments performed in triplicate. The dashed line represents the theoretical graphic region corresponding to an additive effect.

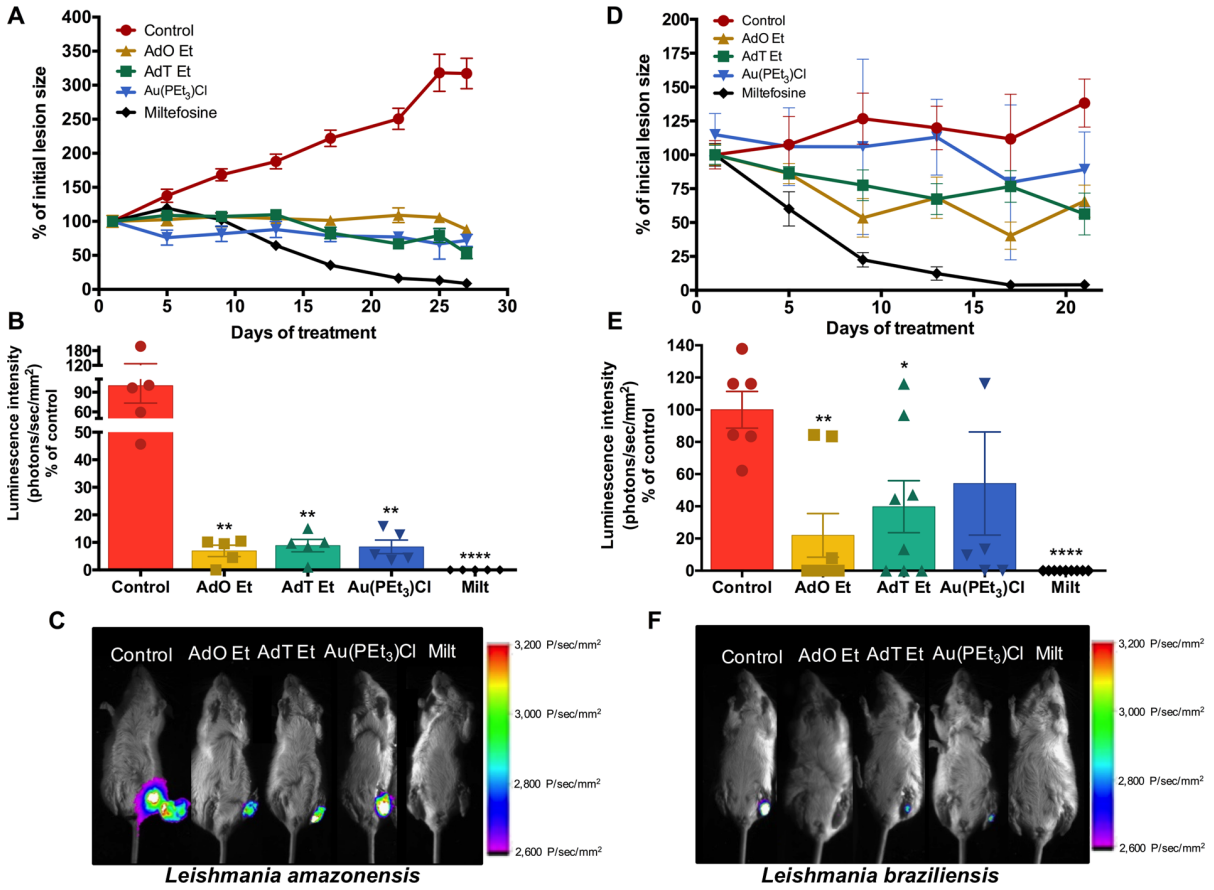

Figure 9. *In vivo* efficacy of gold(I) complexes in BALB/c mice experimentally infected with *Leishmania amzonensis* (A–C) and *Leishmania braziliensis* (D–F). Animals were treated orally with 12.5 mg/kg/day of gold(I) complexes or 15 mg/kg/day of miltefosine (positive control) during 27 or 21 days, respectively, for *L. amazonensis*- and *L. braziliensis*-infected mice. Lesion size was manually measured using a caliper to follow footpad thickness variation (A and D). Luminescence was obtained from a bioimaging assay (B, C, E, and F). For this assay, we used firefly luciferase-expressing *L. braziliensis* (H3227 *Lbr*LUC line) and *L. amazonensis* (PH8 *Lama*LUC line). Experiments were performed twice with at least 4 animals per group for *L. brasiliensis* and 6 animals per group for *L. amazonensis*. Statistical differences between animals treated with $Au(PEt_3)Cl$, AdO, AdT, or miltefosine and the untreated animals were calculated using the Student's *t*-test and one-way ANOVA with multiple comparisons: $*p < 0.05$; $**p < 0.01$; $****p < 0.0001$.

when TR is inhibited or ROS is directly produced, the gold(I) complexes cause oxidative stress in *Leishmania*.

Sb-Resistant *Leishmania* spp. Are Sensitive to Gold(I) Complexes. Since the antileishmanial activity of antimony (Sb) also involves TR inhibition and ROS production,[31,32] we decided to investigate a putative cross-resistance of Sb-resistant (SbR) parasites to gold(I) complexes. This would provide hints on the mechanisms of action and biochemical pathways associated with gold(I) antileishmanial activity. Moreover, the lack of cross-resistance to Sb would further support the development of this new class of metallodrug. For this, sensitivity profiles were performed with gold(I) complexes **1**–**4** on promastigote forms of *L. amazonensis*, *L. guyanensis*, and *L. infantum* and Sb-sensitive (WT) or SbR parasites. The SbR lines did not show cross-resistance. In fact, some were hypersensitive to the gold(I) complexes (Figure 6). AdT Et

https://dx.doi.org/10.1021/acsinfecdis.9b00505
ACS Infect. Dis. XXXX, XXX, XXX–XXX

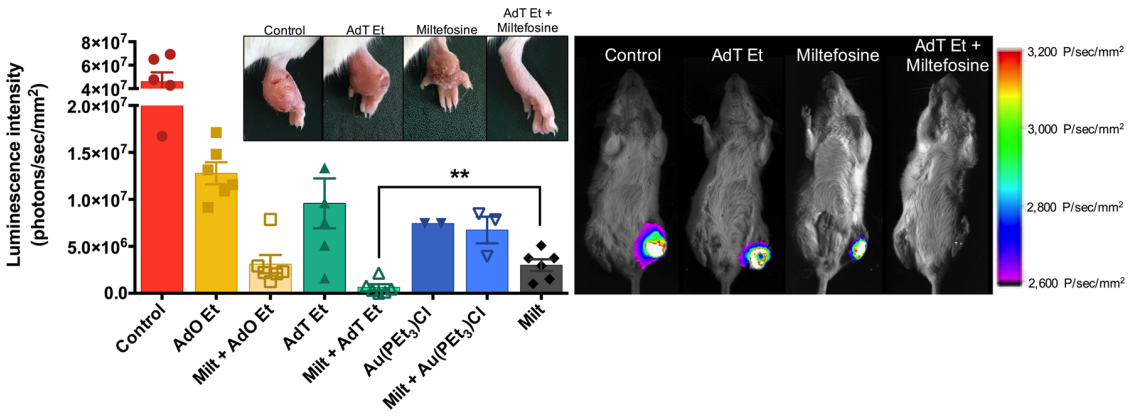

Figure 10. *In vivo* efficacy of the combination of miltefosine and gold(I) complexes in BALB/c mice experimentally infected with *Leishmania amazonensis*. Animals were treated orally with 12.5 mg/kg/day of gold(I) complexes or 15 mg/kg/day of miltefosine during 13 days. Parasite burden was indirectly measured by the luminescence obtained from the bioimaging assay. For this assay, we used firefly luciferase-expressing *L. amazonensis* (PH8 *Lama*LUC line). Differences in lesion appearance on the last day of treatment is pictured above the graph. The experiment was performed once with at least 6 animals per group. Statistical differences between combinations (miltefosine/AdT Et; miltefosine/AdO Et; miltefosine/Au(PEt_3)Cl) and miltefosine alone were calculated using the Student's *t*-test: $^{**}p < 0.01$.

was more active against SbR *L. infantum* when compared with the WT line, in a manner dependent on the complex, since its Au(PEt_3)Cl precursor did not show differences between *L. infantum* WT and SbR lines; a similar pattern was observed for AdO Ph on *L. infantum* (Figure 6A−C,E,F). For triphenylphosphine derivatives, both complexes and their precursor presented higher antileishmanial activity against *L. guyanensis* SbR when compared with their WT counterparts, showing that the free gold(I) precursor is the main pharmacophore in this case (Figure 6D−F).

Gold(I) Complexes AdT Et and AdO Et Decrease Oxygen Consumption of Sb-Sensitive but Not Sb-Resistant *L. infantum*. The evidence of oxidative stress caused by the gold(I) compounds points to possible mitochondrial damage. To evaluate how the gold(I) complexes affect mitochondrial function, we assessed the parasites' respiration profile using an Agilent Seahorse XF Analyzer. When comparing the energy phenotype inherent to *L. infantum* WT and SbR parasites, it was observed that WT cells are more energetic, as they have more oxygen consumption and glycolysis activity, whereas SbR cells are more quiescent, with less respiration activity in general (Figure 7A). This shows that SbR cells already have decreased mitochondrial function when compared to WT. When treated with the complexes for 2 h, WT parasites had an average of a 25% reduction in oxygen consumption (Figure 7B,D), making the cells that were in an energetic state become more quiescent, indicating the impairment of mitochondrial respiration. On the other hand, SbR parasites did not present any alterations in oxygen consumption upon treatment (Figure 7C).

***In Vitro* Combination of AdT Et and AdO Et with Miltefosine Does Not Improve Antileishmanial Activity.** In order to propose an oral combination therapy of drugs with different antileishmanial mechanisms of action, we investigated *in vitro* the physical mixtures of miltefosine with AdO Et and AdT Et. According to the values proposed by Odds[33] for the determination of the synergistic interaction,[33] fractional inhibitory concentration (FIC) values and an isobologram showed that the combination of miltefosine and gold(I) complexes was indifferent, presenting $x\Sigma$FIC of 0.92 and 0.88, respectively (Figure 8). However, the fact that both drugs are not directly interacting with each other does not mean that they could not present an additive antileishmanial effect by their own independent mode of action (e.g., *in vivo*).

AdT Et, AdO Et, and Au(PEt_3)Cl Are Able to Prevent Progression of Cutaneous Leishmaniasis in a Murine Model. BALB/c mice infected with *L. amazonensis* or *L. braziliensis* and treated orally with AdT Et, AdO Et, and Au(PEt_3)Cl presented a reduced lesion size and parasite burden when compared to the untreated control, as revealed by footpad thickness measurements and bioimaging, respectively (Figure 9). In animals infected with *L. amazonensis*, AdT Et and AdO Et treatment reduced parasite burden by 85−100% (Figure 9B). *L. braziliensis*-infected animals presented a more heterogeneous response, as 3 out of 8 animals treated with AdT Et had no detectable parasites and the other 5 had a 50% to 87% reduction in parasite burden or no reduction at all (Figure 9E). For animals treated with AdO Et, 5 out of 8 had no detectable parasites; one had 92% reduction, and the other 2 had 17% of reduction in parasite burden (Figure 9E). Despite the heterogeneity of the results, we observed that in most animals there was a dramatic reduction in lesion size and parasite burden, with many animals having no detectable infection. Therefore, we conclude that the gold(I) complexes are promising compounds for reducing the infection of *L. amazonensis* and *L. braziliensis* in a murine model.

Although Indifferent *In Vitro*, AdT Et and Miltefosine Combination Improves Efficacy, Allowing a Shorter Treatment Scheme *In Vivo*. We performed the *in vivo* drug combination assay of miltefosine and AdO Et, AdT Et, or gold precursor Au(PEt_3)Cl, aiming to reduce the treatment time of miltefosine, one of the major drawbacks associated with the emergence of miltefosine-resistant parasites. In the efficacy studies using *L. amazonensis*, we performed treatment with miltefosine as a positive control for 27 days, with a 50% reduction on mean lesion size occurring around day 13. The combined treatment scheme was designed using the full doses of both drugs (12.5 mg/kg of the gold(I) compounds and 15 mg/kg of miltefosine) for 13 days. At the end of the treatment, miltefosine alone had reduced the mean lesion size by 45% and miltefosine combined with AdT Et had reduced it by 65%. The parasite burden was also significantly reduced by the

https://dx.doi.org/10.1021/acsinfecdis.9b00505
ACS Infect. Dis. XXXX, XXX, XXX−XXX

combination with AdT Et, where the animals treated with the miltefosine + AdT Et combination exhibited 80% less luminescence, and therefore parasite burden, than miltefosine alone (Figure 10).

Au Serum Levels in Mice Last for Days upon Gold(I) Oral Treatment. The study of the pharmacokinetic properties of the gold(I) complexes is important for better understanding the efficacy and toxicology results and the effect of the different ligands *in vivo* and to help improve treatment schemes. Our results showed that the precursor is more rapidly absorbed and lasts longer in the serum than the complexes AdT Et and AdO Et (Table 3). The absorption half-life phase follows $Au(PEt_3)Cl$ > AdT Et ≫ AdO Et, while the half-life elimination time favors long-term permanence and slow clearance of the free precursor, where AdT Et > AdO Et ≫ $Au(PEt_3)Cl$ (Table 3).

Table 3. Pharmacokinetic Parameters of Gold(I)-Derived Compounds in BALB/c Mice Treated Orally with a Single Dose of 12.5 mg/kg[a]

compound	C_{max} (mg/L)	T_{max} (h)	MRT (h)	AUC (mg·h/L)	$T_{1/2}$ (abs) (h)	$T_{1/2}$ (el) (h)
AdT Et	2.42	10.82	32.08	105.0	5.35	18.36
AdO Et	2.30	12.25	55.98	202.3	3.86	35.93
$Au(PEt_3)Cl$	4.00	6.89	79.69	345.8	1.47	54.31

[a] C_{max}: maximum Au serum concentration; T_{max}: time for reaching Au peak serum concentration; MRT: Au mean residence time projected to infinity; AUC: area under the Au serum concentration/time curve projected to infinity; $T_{1/2}$ (abs) and $T_{1/2}$ (el): Au absorption and elimination phase half-life.

Although orally administered by gavage at 12.5 mg/kg/day, gold(I) complexes AdT Et and AdO Et reached only 2.4 and 2.3 mg/L, respectively, in mice serum, which was enough to exert antileishmanial activity. Although they present different absorption times, AdO Et and AdT Et achieve a similar maximal concentration (Table 3). Despite the higher AUC of precursor $Au(PEt_3)Cl$ at 345.8 mg·h/L, we could not associate it with *in vivo* efficacy (Figure S4), which prompted us to investigate BSA binding and toxicity.

Gold(I) Complexes Possess a High Affinity for Albumin, AdO Et-BSA Being More Stable than AdT Et-BSA. As gold is reported to bind albumin and we observed remarkably long $T_{1/2}$ (el) times (Table 3), we decided to investigate how the compounds specifically bind to albumin. The complexes display a decrease in the intensity of the BSA fluorescence signal as a function of increasing concentration, without changes in the emission maximum or in the shape (Figure 11A–C). This implies a change in the microenvironment around the chromophore of BSA. It is well-known that quenching occurs through a static or dynamic process, both of which can result in a linear Stern–Volmer plot. According to eq S2, the apparent binding constants (K_b) were calculated from the interception and the number of binding sites (n), by the slope. Values of n below 1 (ranging from 0.6 to 1) indicate that there is approximately one class of binding sites for the gold complexes toward BSA (Figure 11D). Data acquired at 35 °C are shown in Figure 11D. The precursor has the highest binding constant ($K_b = 1.46 \times 10^3$ M^{-1}) and class of binding sites ($n = 0.95$) compared to AdO Et ($K_b = 0.89 \times 10^3$; $n = 0.87$) and AdT Et ($K_b = 0.19 \times 10^3$; $n = 0.60$). For the precursor $Au(PEt_3)Cl$, the K_{sv} variation is at the error range and the thermodynamic parameters could not be determined

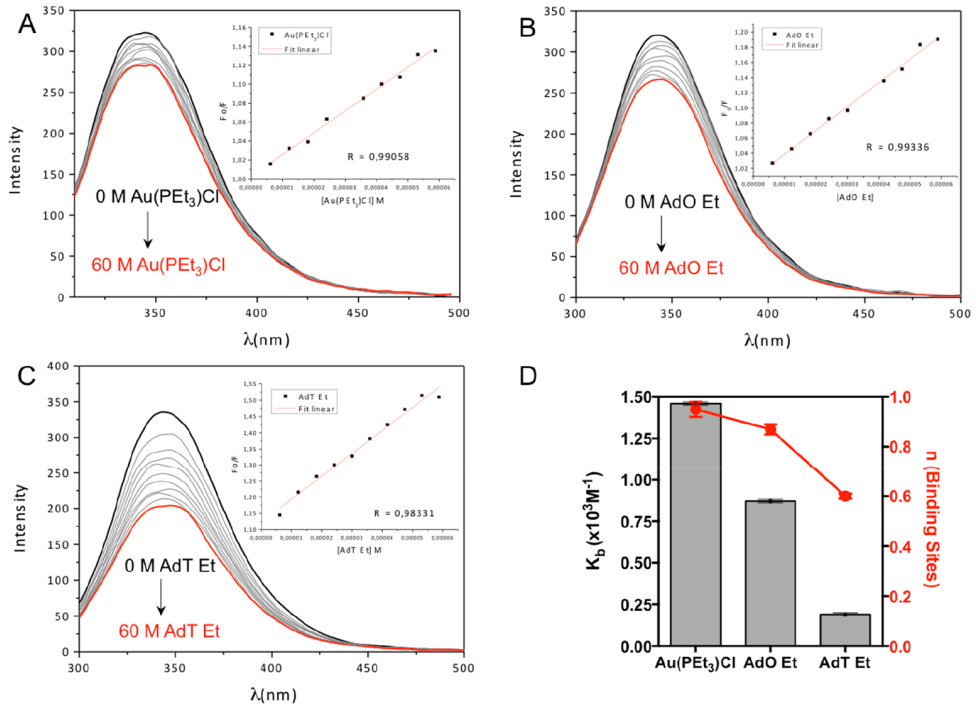

Figure 11. Fluorescence quenching emission spectra of BSA in the absence and presence of gold(I) compounds. Precursor (A), AdO Et (B), and AdT Et (C) ([BSA] = 1.0 μM and [gold compound] = 0–60 μM). Binding constant (K_b) and number of protein biding sites (n) at 35 °C (D) for gold compounds; data highlighted in Table S3. The fluorescence intensities of the Tris–HCl and the gold complexes were irrelevant under experimental conditions.

https://dx.doi.org/10.1021/acsinfecdis.9b00505
ACS Infect. Dis. XXXX, XXX, XXX–XXX

Table 4. Biochemical Parameters for the Evaluation of Nephro- and Hepatotoxicity of Mice Treated with Saline + 10% of DMSO (Vehicle), AdT Et, AdO Et, Au(PEt_3)Cl, or Miltefosine for 27 Days[a]

	compound				
parameter	vehicle	AdT Et	AdO Et	Au(PEt_3)Cl	miltefosine
ALT (mg/dL)	36 ± 10	28 ± 2	40 ± 7	41 ± 14	37 ± 6
AST (mg/dL)	110 ± 20	92 ± 12	106 ± 18	124 ± 38	109 ± 30
urea (U/L)	59 ± 2	59 ± 5	63 ± 9	68 ± 9	60 ± 9
creatinine (U/L)	0.38 ± 0.04	0.36 ± 0.04	0.38 ± 0.08	0.33 ± 0.02	0.64 ± 0.16[b]

[a]ALT: alanine aminotransferase; AST: aspartate aminotransferase. Data were expressed as mean ($n = 6$) ± standard deviation of the mean. Gold(I) compounds were administered orally at a dose of 12.5 mg/kg/day and miltefosine, at 15 mg/kg/day. [b]Statistical significance between vehicle control and drug treatment. Student's t-test with $p < 0.05$ was considered significant.

since linear regression did not return a favorable correlation coefficient (R^2). K_{sv} and K_b values decrease with increasing temperature for AdO Et, suggesting a static interaction. On the other hand, AdT Et-BSA presents a dynamic interaction process in which K_{sv} values increase with temperature (Table S3).

AdT Et, AdO Et, and Au(PEt_3)Cl Are Not Nephrotoxic or Hepatotoxic for Mice during 27 Day Treatments. At the end of the efficacy assay, mice treated with the gold(I) complexes had nephrotoxicity and hepatotoxicity evaluated biochemically. We did not observe any signs of toxicity in the animals treated with AdT Et or AdO Et throughout the experiment; however, about 50% of the animals treated with Au(PEt_3)Cl died from toxic effects. At the end of the treatment, all levels of urea, creatinine, ALT, and AST were normal, as compared to untreated control, even for the survivors of the treatment with Au(PEt_3)Cl (Table 4). In contrast, animals treated with miltefosine showed signs of nephrotoxicity as they presented a 68% increase in creatinine levels (Table 4), reinforcing the importance of reducing miltefosine treatment time with combination therapy.

DISCUSSION

We evaluated the antileishmanial activity of four gold(I)-based complexes and explored the mechanisms of action and *in vivo* efficacy of the two most active compounds. All tested gold(I) complexes presented potent antileishmanial activity. Since ligands alone are not active, the precursors are essential for the bioactivity, with the triethylphosphine-derived complexes possessing more pronounced activity than those using triphenylphosphine as precursors. It corroborates previous data from our group, where triethylphosphine-derived gold(I) complexes were more active than triphenylphosphine-substituted ones.[19] This effect has been overcome in *Leishmania* spp. intracellular amastigotes exposed to tiazolidine-substituted gold(I) complexes, highlighting the importance of this ligand for a putative host-dependent pharmacodynamics. Superior antitumoral activity was also observed for triethylphosphine-based complexes.[28] Considering that anticancer agents can be active against parasites,[19,34] it supports the strategy of drug repurposing as a tool to develop and improve the antileishmanial chemotherapeutic arsenal. The complexes were more active against intracellular amastigotes than promastigotes, suggesting that host cells somehow participate in their mode of action. Adamantane-derived gold(I) complexes were selected for further investigations on the basis of the high antileishmanial activity, despite the low SI values, supported by the urgent need for alternatives to treat leishmaniasis.

Adamantyl is a lipophilic group, usually found in substances presenting antimicrobial, antiviral, and anticancer activities.[28,35] The adamantyl group could have increased the antileishmanial activity of the complexes by increasing their lipophilicity or by exerting biological activity itself.

Auranofin is able to inhibit TR;[27] thus, it is one of the putative mechanisms of action of gold(I) complexes. Few complexes are able to selectively inhibit TR, and several TR inhibitors identified by enzymatic assays or docking studies do not present satisfactory antiparasitic activity.[36,37] Adamantane-derived complexes presented potent TR inhibition, superior to that of Sb^{III},[37] the main active agent used worldwide to treat all forms of leishmaniasis, despite drawbacks including toxicity and the emergence of parasitic resistance.[31] Because of its selectivity, TR inhibition is still one of the main targets for drug development against leishmaniasis.[38] Since we performed the enzymatic inhibition assay using *T. cruzi*-derived *Leishmania* spp. homologous TR, we validated by docking that the gold(I) complexes are able to inhibit the *Leishmania* enzyme as well. Almost all *T. cruzi* TR residues that are involved in trypanothione binding are conserved in *L. infantum* TR, as previously demonstrated.[31] Therefore, we can deduce that the binding of other ligands will occur in a similar way in both enzymes. Moreover, we could observe that the adamantane and phosphine hydrophobic ligands have the function to orientate the docking, putting the gold center close to the redox-reactive site Cys52(A). The docking pose favors the reaction of Cys52(A) with the gold metal, releasing the thiazolidine ligand. We showed previously that such ligand-exchange reactions should proceed quickly and faster for AdT than for AdO.[28] Indeed, in the functional TR inhibition assay, the precursors (without adamantane) were already able to inhibit the enzyme. Despite the importance of TrxR for gold(I) complexes, human gluthathione reductase (GR) is the nearest candidate homologue of TR with around 40% sequence identity.[39] However, both have enough differences in their active sites for the specific NADPH-dependent reduction of the disulfide substrate. Moreover, it was proven by different approaches that TR is essential for *Leishmania* and *Trypanosoma*.[40−42] This is strong evidence that TR can be considered a good target for druggable selective inhibitors.

When the technical limitations were considered, our results showed that the complexes AdT Et and AdO Et were associated with increased intracellular ROS, indicating that oxidative stress is likely involved in gold(I)'s mode of action. An increased ROS accumulation was observed in tumoral cells treated with gold(I) complexes.[7,43,44] It is worth noting that precursor Au(PEt_3)Cl causes DNA damage, which is somehow prevented in the case of gold(I) complexes AdT Et and AdO Et. This finding fits with the high toxicity observed by the

https://dx.doi.org/10.1021/acsinfecdis.9b00505
ACS Infect. Dis. XXXX, XXX, XXX−XXX

triethylphosphine gold(I) precursor *in vivo* together with long-term blood clearance due to the high affinity for serum albumin.

Among the known mechanisms of action of Sb-based drugs, TR inhibition and ROS generation[32] are shared with gold(I) complexes, raising the concern of cross-resistance between these compounds. However, SbR mutants from *L. infantum*, *L. guyanensis*, and *L. amazonensis* were not cross-resistant upon treatment with adamantane-based gold(I) complexes.

In fact, some SbR populations were more sensitive to the complexes, indicating that the biochemical adaptations achieved for SbR mutants to become resistant did not affect the gold(I) targets. Other studies already demonstrated that drug resistant parasites may suffer random mutations resulting from the resistance selection process that affects their sensitivity to other drugs and overall proficiency.[45−47] Indeed, we found that SbR parasites presented a low respiration profile when compared to the more energetic WT parasites. This result corroborates the fact that resistant parasites may become less proficient. Gold(I) complexes, as expected, decreased oxygen consumption in WT parasites, indicating an early onset of mitochondrial dysfunction. Diversely, SbR parasites did not present any alterations in their respiration profile upon treatment, indicating that the hypersensitivity of these parasites to the gold(I) complexes occurs by a different mode of action. These observations demonstrate that gold(I) complexes not only are potential drug candidates for leishmaniasis caused by antimonial resistant parasites but also can be used as a pharmacological tool for the study of drug action and resistance mechanisms in *Leishmania*.

In our work, we used this technique to obtain insights into the structure−activity relationship of the gold(I) complexes. The use of EDX in the intracellular quantification of gold(I) complexes for the mechanism of action study was reported in a study using triethylphosphine gold(I) chloride; however, the authors did not obtain a Au signal in their samples.[48] Our success in only detecting $Au(PPh_3)Cl$-derived complexes and not $Au(PEt_3)Cl$ suggests that triphenylphosphine promotes a greater incorporation of these complexes (Figure S3). The compounds containing the triphenylphosphine precursor are more lipophilic, with logP of 6.81 (AdO Ph) and 7.23 (AdT Ph) against 5.19 (AdO Et) and 5.45 (AdT Et) of the triethylphosphine compounds. This feature increases the ability of these compounds to cross cell membranes. The triphenylphosphine-derived precursor seems to play a role on gold(I) cell distribution, since we were not able to detect Au by EDX upon exposure to AdO Et at 1 mM for 3 h. Despite their higher lipophilicity, $Au(PPh_3)Cl$ complexes are less active; hence, the presence of triphenylphosphine likely inhibits the binding of the complex to its specific target. We also evaluated the Au uptake by *Leishmania* promastigotes using atomic absorption spectroscopy; however, adsorption control cells (exposed to gold(I) complexes at 4 °C, immediately washed, and digested for reading) showed similar Au amounts to those obtained after 30 min or 1 h of incubation (Figure S5), making this approach not suitable to precisely infer about the uptake of gold(I) complexes.

In vivo efficacy assays revealed that the oral treatment with AdT Et and AdO Et, even in low doses, is able to reduce lesion size and parasite burden in cutaneous leishmaniasis animal models. New antileishmanial candidates for oral administration are usually tested around 50 mg/kg,[49−51] highlighting how the gold(I) complexes studied here are promising antileishmanial drugs. Since gold(I) complexes are known to possess anti-inflammatory properties,[52−54] we speculate that this feature could serve synergistically with their antileishmanial activity to treat experimental leishmaniasis. The combination of AdT Et with miltefosine, although not indicative of the synergic effect *in vitro*, had encouraging results *in vivo*, showing improved reduction in parasite burden with half the treatment duration. The same pattern was previously found for the combination of miltefosine and the anticancer drug tamoxifen.[55] Miltefosine has been successfully used in several combination treatment studies with drugs already in use for leishmaniasis such as amphotericin B[56] and new bioactive substances.[57−60]In the study performed by Sharlow et al.,[26] Balb-c mice were infected with *L. major* and treated with auranofin by the IP route at 20 mg/kg/day for 10 days, either 3 days after infection or after a footpad lesion was established. Even using higher doses and a more invasive route of administration than us, they still saw an increase in lesion size over time in mice that were treated after the disease was established. Although the increase was lower than in the untreated mice, auranofin was not sufficient to control the disease progress. Our compounds showed higher inhibition profiles at lower oral doses and in a model that is a lot more aggressive (*L. amazonensis* and Balb-c). Here, the *in vivo* efficacy study revealed that 12.5 mg/kg/day of AdT Et combined with 15 mg/kg/day of miltefosine for 13 days was able to clinically cure the mice with almost zero parasite burden. As for safety, auranofin has extensive preclinical and clinical data that demonstrates its safety. The toxicity data we showed in this paper for our compounds are not as extensive, but we were able to demonstrate that the compounds have a good therapeutic window and low toxicity even though they are administered orally with no special formulation that could further improve the safety. When compared to its gold(I) precursor, AdT Et was less toxic and all animals in the group survived, evidencing a protective role *in vivo* by the adamantane ligand.

The gold complexes studied here have a high affinity to albumin and, therefore, have long half-lives in the murine model. One possibility to improve the efficacy of these complexes would be to administer fewer but higher doses. Another interesting observation derived from the Pk (pharmacokinetics) data is that the precursor has a higher and earlier concentration peak, takes longer to be eliminated, and is also more toxic for the animals. This allows for the conclusion that the ligands decrease the affinity of the complexes to albumin and, as a consequence, they are less toxic.

Garcia et al. previously reported the influence of BSA in the cytotoxicity for AdT Et and AdO Et *in vitro*.[28] The affinity of gold complexes to BSA is directly related to K_b values. At 35 °C, the gold−BSA interactions increase from AdT Et to the precursor. These results are consistent with the Pk parameters and explain the difference of $T_{1/2}$ (elimination) and AUC (Table 3); the higher the K_b, the higher are $T_{1/2}$(elimination) and AUC. The reported K_b value for cisplatin is similar: 8.52×10^2 M^{-1} [59] for human serum albumin. Other gold complexes are higher, around 10^3−10^4 M^{-1} [60,61] and even higher values were reported for gold nanoparticles (10^6−10^{10} M^{-1}).[62,63] The moderate values of binding constants in our complexes could indicate that they can be stored and carried by this protein and easily released. Coffer et al. investigated auranofin and its precursor $Au(PEt_3)Cl$ for BSA interactions using ^{31}P NMR. They concluded that the Cl^- can be replaced by a 34-Cys

https://dx.doi.org/10.1021/acsinfecdis.9b00505
ACS Infect. Dis. XXXX, XXX, XXX−XXX

residue or other ligands from albumin. However, this results in a weaker Au−Cl bond compared to the Au−SR bond in auranofin.[64]

Finally, the biochemical markers for nephrotoxicity and hepatotoxicity showed that animals treated with the complexes had no alterations in kidney and liver function when compared to untreated animals. Gold complexes are often associated with nephrotoxicity and hepatotoxicity, leading to narrow therapeutic indexes.[65] Although we observed toxicity when the complexes were administered using higher doses or intraperitoneally (data not shown), oral treatment with 12.5 mg/kg was enough to exert antileishmanial activity without remarkable toxicity. These results encourage us to develop the adamantane-derived gold(I) complexes as new drug candidates to treat leishmaniasis. A brief analysis on the costs of AdT Et as a drug candidate to treat leishmaniasis, based on the material costs, synthesis, and animal/human dose extrapolation,[66] revealed a value of around USD 200 per patient/treatment, which is affordable when compared to the current therapies using meglumine antimoniate, amphotericin B, and miltefosine with costs of USD 418.52, 13,243.48, and 200−51,000, respectively.[67−70]

CONCLUSIONS

The data shown here demonstrates that gold(I) complexes are promising drug candidates to treat leishmaniasis. The mode of action of these chemical entities involves oxidative stress by direct ROS production or their indirect accumulation due to TR inhibition and mitochondrial damage. These complexes are also relevant in the development of medicines to treat leishmaniasis caused by antimony-resistant parasites. Treatment with AdT Et and AdO Et was effective for experimental cutaneous leishmaniasis. The combination of AdT Et and miltefosine improved treatment outcomes and could be explored to decrease the duration of miltefosine treatment, reducing the chances of selecting resistant parasites. The presence of the ligands decreases toxicity, possibly by decreasing the compounds' affinity to albumin. Therefore, AdT Et and AdO Et can be considered leads in the development of new antileishmanial drugs highlighting chrysotherapy as a feasible strategy for leishmaniasis treatment.

METHODS

Chemicals and Synthesis of Gold(I) Complexes. Precursors chloro(triethylphosphine)gold(I), $Au(PEt_3)Cl$, and chloro(triphenylphosphine)gold(I), $Au(PPh_3)Cl$, were purchased (SigmaAldrich #288225 and #254037). The synthesis of gold(I) complexes was performed and described in previously published work.[28,71] All compounds had purity (>95%) confirmed by the melting point, elemental analysis, and mass spectrometry (Supporting Information).

Parasite Strains. *Leishmania (Viannia) braziliensis* (MHOM/BR/1975/M2904 and MHOM/BR/1994/H3227), *Leishmania (Leishmania) infantum* (MHOM/MA/1967/ITMAP-263 and MCAN/BR/2000/BH400), *Leishmania (Viannia) guyanensis* (MHOM/BR/1975/M4147), and *Leishmania (Leishmania) amazonensis* (MHOM/BR/1989/Ba199 and IFLA/BR/1967/PH8) were maintained in minimum essential culture medium (α-MEM) supplemented with 10% (v/v) heat inactivated FBS (Cultilab, Campinas, SP, Brazil), 100 mg/mL kanamycin, 50 mg/mL ampicillin, 2 mM L-glutamine, 5 mg/mL hemin, and 5 mM biopterin (Sigma-Aldrich, St Louis, USA) at pH 7.04 and incubated at 25 °C. Strains of *L. braziliensis* H3227 (*Lbr*LUC) and *L. amazonensis* PH8 (*Lama*LUC) with a genomic DNA copy of firefly luciferase as a reporter gene were engineered as previously reported.[72,73]

Antipromastigote Activity. Log phase promastigotes (1×10^6 parasites/mL) were seeded in 24-well cell culture plates containing 1.5 mL of α-MEM and incubated while shaking at 25 °C for 72 h in the presence of several concentrations of gold(I) complexes. Controls were performed using cultures in the presence of amphotericin B and miltefosine. Nontreated parasites were established for growth comparison. Stock solutions of gold(I) complexes were dissolved in DMSO and diluted in α-MEM cell culture medium to obtain the range of tested concentrations. The final DMSO concentration did not exceed 1%, which is known to be nontoxic to *Leishmania* parasites.[74] For drug susceptibility assays, *Leishmania* growth curves were constructed by measuring absorbance at 600 nm on a Spectramax M5 (Molecular Devices).[75] The antileishmanial activity is expressed as IC_{50}/72 h, which is the concentration that reduces cell growth by 50% compared to the untreated control (growth inhibition). Antimony-resistant *Leishmania* spp. were previously selected by *in vitro* stepwise selection,[76] where promastigote forms are exposed to an increased drug concentration until they achieved a growth pattern similar to the wild-type counterparts. Resistance indexes were then obtained on the basis of drug sensitivity profiling curves.

Antiamastigote Activity. For this assay, we used *L. braziliensis* (MHOM/BR/1994/H3227) and *L. infantum* (MHOM/MA/1967/ITMAP-263) parasites expressing firefly luciferase as a reporter gene (pSP72αHYGαLUC1.2), *Lbr*LUC and *Lin*LUC. Transfections were performed as previously described.[77] Human monocyte-derived macrophage cell line THP-1 was maintained in RPMI 1640 medium supplemented with 10% FBS. Cells were plated in blank 96-well tissue culture plates at 8×10^5 cells/mL and differentiated by incubating with 20 ng/mL of Phorbol 12-myristate 13-acetate (PMA; SigmaAdrich, #P8139) at 37 °C in a humid atmosphere containing 5% CO_2 for 3 days. Cells were washed with RPMI medium and subsequently infected with *Lbr*LUC or *Lin*LUC at a parasite/macrophage ratio of 10:1 for 3 h. Noninternalized parasites were removed by three washes with HEPES/NaCl buffer (20 mM HEPES, 0.15 M NaCl, 10 mM glucose, pH 7.2). After 3 days, the RPMI medium was aspirated and the luciferase activity assessed by adding 20 μL of reconstituted One-Glo Luciferase Assay System solution as enzyme substrate, following the manufacturer's instructions (Promega, Madison, WI, USA #E6110). Luciferase activity was measured by luminescence detection in a luminometer SpectraMax M5 (Molecular Devices, Sunnyvale, CA, USA) using a 1 s integration/well. Noninfected THP-1 macrophages were considered as the signal background, while nontreated infected THP-1 cells were used as a control for growth comparison. Amphotericin B and miltefosine were added as a positive control. The strains used for intracellular amastigote assays and *in vivo* experiments were periodically passaged in mice and not used for more than 10 passages (for *in vivo* experiments, infections were performed with parasites recently isolated).

Cytotoxicity Assay. The *in vitro* cytotoxicity activity was evaluated by quantifying the ability of THP-1 macrophages to reduce the yellow dye 3-(4,5-dimethyl-2-thiazolyl)-2,5-diphenyl-2*H*-tetrazolium bromide (MTT, Sigma-Aldrich #M2128) to

https://dx.doi.org/10.1021/acsinfecdis.9b00505
ACS Infect. Dis. XXXX, XXX, XXX−XXX

a purple formazan product.[78] For THP-1 macrophage differentiation, 2×10^5 precursor monocytes/well treated with 20 ng/mL PMA were seeded in 96-well plates and incubated for 3 days at 37 °C in a 5% CO_2 humid atmosphere. Stock solutions of gold(I) complexes were prepared in DMSO and serially diluted in RPMI medium (<1% DMSO). After 72 h of drug exposure at 37 °C and 5% CO_2, cells were incubated with MTT (10 mM in a water solution, 20 μL/well) for 4 h at 37 °C and 5% CO_2. MTT is metabolized by viable cells resulting in a purple product that after being solubilized in 100 μL of DMSO and can be quantified by measuring the absorbance at 570 nm using a plate reader Spectramax M5 (Molecular Devices). The negative control was performed using untreated cells in RPMI 1640. Amphotericin B and miltefosine were added as a positive control.

Trypanothione Reductase Inhibition Assay. This assay is a colorimetric-based test where TcTR (TSHR) recycles the reduced form of its substrate trypanothione, which reacts with DTNB [5.5′-dithiobis(2-nitrobenzoic acid)], forming the yellow detectable 2-nitro-5-thiobenzoate anion (TNB) that can be measured at 412 nm.[79] The assay was performed using recombinant trypanothione reductase from *T. cruzi* (TcTR) expressed in *Escherichia coli* BL21DE3 and purified by affinity chromatography. TR assays were performed as described by Hamilton et al.[79] in 96-well flat bottom micro plates at a final volume of 240 μL containing 40 mM HEPES (pH 7.5), 1 mM EDTA, 150 μM NADPH, 1 μM trypanothione (Bachem, Torrance), 25 μM DTNB (Sigma-Aldrich #D8130), 40 ng TcTR, and 100 μM gold(I) complexes **1**, **2**, **3**, and **4** in DMSO. Clomipramine (Sigma-Aldrich #C-116) was used as a positive control and the vehicle DMSO (1%), as a negative control. The mixture was preincubated at 27 °C for 30 min, and after 10 μL of DTNB was added, the absorbance was read at a λ of 412 nm for 30 min in 5 min intervals in a TECAN Infinite M200 micro plate reader. All assays were done in triplicate and repeated twice.

Docking. The *Leishmania infantum* TR (PDB code 2JK6) was selected as the receptor for docking. The binding site was defined from the list of residues interacting with trypanothione,[80,81] which include Ser14-Asn22; Cys52-Leu62; Val102-Phe114; Leu334-Gly342 (monomer A) and Ser395-Leu399; Val460-Ser470 (monomer B). The crystallographic waters were removed, and the protein was protonated according to the physiological pH. The ligand structures (gold complexes) were taken from our previous paper.[28] The search for the best docking poses was carried out using a genetic algorithm (GA) with all parameter settings in the automatic mode and 200% search efficiency in the GOLD program,[82] recommended for flexible ligands. Each ligand was docked 50 times starting from different orientations, and the obtained poses were ranked by the ChemPLP fitness function.[83] The Cys52 and Cys57 are directly involved in the enzyme activity and are potential targets for Au(I) complexes. Therefore, the inhibition of the TR enzyme by the gold complex is expected to occur through a covalent binding of Au−S, and both species must be close enough for the reaction to take place. In docking experiments, a chemical reaction is not possible. To simulate the prereaction step, we constrained the Au···S (Cys52(A)) distance within the range of 1.5−3.5 A, which covers the Au−S distance (∼2.5 A) in transition states for the reaction of Au(I) complexes with Cys.[84] In the GOLD program, the distance constraint applies as a penalty in the fitness score calculated as $E = kx^2$ when the specified distance is found outside of the distance bounds. It is also worth mentioning that the scoring functions available in the GOLD software do not account for heavy metal parameters; therefore, the previous boundary condition is necessary to make docking possible and avoid spurious results. The last assumption made was to fix the C−S bond, avoiding the syn-anti conformational change. In our previous paper,[28] we showed that the antiform is at least 3 kcal mol^{-1} more stable than the syn form in a solution that is in agreement with the crystal structure. Moreover, the conformational interconversion is expected to be sterically forbidden in the enzyme binding site. The computation of charge distribution and generation of an electrostatic profile were performed using the APBS software,[85] version 1.9.

ROS Measurement. For assessing the levels of ROS, *L. braziliensis* promastigotes were harvested from mid log phase and exposed to three different oxidant-sensitive probes. Cells were washed with HEPES/NaCl, resuspended in HEPES/NaCl containing 20 μM H_2-DCFDA (2′,7′-dichlorodihydrofluorescein diacetate) (ThermoFischer #D399) and seeded at 5×10^6 cells/well as previously reported.[86] Cells were either left untreated or treated with the IC_{50} of gold(I) complexes for 2 h. Exposure to 1 mM H_2O_2 was performed as the positive control. Fluorescence was measured with a fluorometer SpectraMax M5 (Molecular Devices) at 485 nm excitation and 530 nm emission wavelengths. ROS levels were determined by comparing the values obtained for treated cells with the values obtained for untreated cells. For CellROX Deep Red (Thermo Fisher Scientific #C10422) and CellROX Green (Thermo Fisher Scientific #C10444) assays, *L. braziliensis* promastigotes were treated for 2 h with the IC_{50} of each compound, left untreated, or exposed to 100 μM H_2O_2 (positive control). After treatment, 1×10^7 parasites were collected and washed twice with a 1× PBS solution, followed by incubation with 5 μM CellROX Deep Red or CellROX Green reagents during 30 min at 28 °C. Parasites were washed twice with 1× PBS, and fluorescence was quantified by flow cytometry using a BD Accuri C6 Flow Cytometer (BD Biosciences). All experiments were performed in triplicate. For fluorescence microscopy analysis, the same protocol was used, and after CellROX Green reagent treatment, parasites were seeded in a poly-L-lysine coated slice, stained with DAPI for 20 min, and used for image acquisition with an Olympus (BX-61) microscope, followed by blind deconvolution employing the AutoQuant X2.2 software (Media Cybernetics). A cell-free assay for an auto-oxidation control was performed by incubating the probe with the gold(I) complexes. No signal was detected (data not shown).

Cellular Respiration Assay. The oxygen consumption rate (OCR) and extracellular acidification rate (ECAR) were analyzed in a Seahorse XFe96 Analyzer (Agilent Technologies). The day before the experiment, the Agilent Seahorse XFe96 Sensor Cartridge was hydrated with 200 μL/well of XF calibrant solution overnight in a non-CO_2 incubator at 37 °C. On the day of the experiment, 100 mL of Seahorse assay medium was prepared, containing 1 mM pyruvate, 2 mM glutamine, and 5 mM glucose. The pH of prewarmed (37 °C) medium was adjusted to 7.4 with 0.1 N NaOH. *L. infantum* (MCAN/BR/2000/BH400) sensitive (WT) and antimony (Sb)-resistant (SbR) strains were seeded in 96-well plates at 5×10^5 parasites/well and exposed for 2 h to 2× the IC_{50} of the gold(I) complexes. Cells were then transferred to a Seahorse specific cell culture microplate pretreated with 50 μL of poly-L-lysine in 175 μL of the respective Seahorse medium per well.

https://dx.doi.org/10.1021/acsinfecdis.9b00505
ACS Infect. Dis. XXXX, XXX, XXX−XXX

Plates were centrifuged at 200*g* for 1 min, and OCR and ECAR measurements were performed in 5 min intervals for 30 min to determine basal respiration. The experimental design was set up using the WAVE software, and measurements were performed in the Seahorse XFe96 Analyzer. The cellular respiratory assay was inspired in the bioenergetic profiling of the *Leishmania*-related trypanosomatidae parasite, *Trypanosoma cruzi*, published by Shah-Simpson et al.[87] Briefly, bioenergetic profiling is inferred in the presence of mitochondrial respiratory chain complex inhibitors that are sequentially injected through ports in the Seahorse flux pack cartridges, such as 2 μM oligomycin (inhibitor of ATP synthase complex V), 1 μM carbonyl cyanide-4-(trifluoromethoxy)phenylhydrazone (FCCP - protonophoric uncoupler), and 1 μM antimycin A (complex III inhibitor) The nonmitochondrial respiration is the oxygen consumption in the presence of antimycin A (or rotenone, a complex I inhibitor). Maximal respiration is the basal OCR in the presence of FCCP, while respiratory capacity (or spare capacity) is the maximal respiration (OCR + FCCP) minus basal (OCR without FCCP).[88] Although, Shah-Simpson and et al.[87] were able to optimize the system and demonstrate that the extracellular flux XFe Seahorse technology can be utilized to analyze *T. cruzi* mitochondrial bioenergetics, we were not able to reproduce the same pattern in *Leishmania* spp. promastigotes (data not shown) that responded differently to the inhibitors. However, the basal OCR and ECAR values were consistent and used to compare WT and SbR backgrounds in the presence or absence of gold(I) complexes. A similar approach, focused only on basal OCR, was previously published using *T. cruzi*.[89]

Determination of Drug Interactions. To evaluate whether gold(I) complexes have synergistic interactions with miltefosine, the modified isobologram method was used.[90] Concentration−response curves and predetermined IC_{50} values were used to define the maximum concentrations of each drug. Maximum concentrations were prepared in ratios of 100:0, 80:20, 60:40, 40:60, 20:80, and 0:100 of AdT Et or AdO Et and miltefosine, respectively, followed by 5 serial dilutions (base 2). The drug IC_{50} was calculated for each combination ratio, and the fractional inhibitory concentrations (FICs) were calculated using the ratio of the IC_{50} value of the drug in combination and the IC_{50} of the drug alone. The sum of FIC (ΣFIC) was calculated by the sum of the FIC for each drug in each ratio (e.g., FIC drug A + FIC drug B in proportion 80:20). The mean ΣFIC (xΣFIC) was calculated as the average of ΣFIC and used to classify the interaction as recommended by Odds:[33] synergistic interaction for $x\Sigma\text{FIC} \leq 0.5$, no interaction for $0.5 < x\Sigma\text{FIC} < 4$, and antagonistic interaction for $x\Sigma\text{FIC} > 4$. Isobolograms were built by plotting the FIC for each drug ratio. For details, see Table S1.

***In Vivo* Efficacy Assay.** *In vivo* experiments were performed in female BALB/c mice (4−5 weeks old) inoculated with 1×10^6 stationary phase *Lbr*LUC or *Lama*LUC promastigotes subcutaneously into the hind right footpad (final volume 30 μL). Five weeks after infection, lesion size was evaluated and mice were distributed in homogeneous groups of five to seven animals with equivalent mean lesion sizes. Animals received the treatment with gold(I) complexes orally in a 1% methyl cellulose (SigmaAldrich #M7027) solution for 21 consecutive days for infections with *Lbr*LUC or 27 days for infections with *Lama*LUC. The dose of 12.5 mg/kg/day was chosen after the preclinical acute toxicity evaluation. Treatment outcome was determined through lesion growth and parasite burden at the end of treatment. Lesion growth measurements were obtained using a caliper (Mitutoyo Corp., Japan). Parasite load was determined through luciferase detection by bioimaging (*In Vivo* Xtreme, Bruker, Billerica, MA, USA) as previously described.[91] Briefly, bioimaging was acquired 20 min after luciferin intravenous administration (75 mg/kg of VivoGlo Luciferin, *in vivo* grade, Promega #P1041). Images were taken in high-resolution mode with an exposure of 2 min from a fixed-size region of interest. Results were expressed as the number of photons/s/mm^2. Assays involving the use of animal models were previously approved by the Ethics Committee for Animal Use (CEUA/Fiocruz, LW-5/18) and are according to the Guide for the Care and Use of Laboratory Animals (NRC).

Pharmacokinetics. Groups of 4 to 9 female BALB/c mice (4−5 weeks old) were treated orally with 12.5 mg/kg of gold(I) complexes. After 10 min, 30 min, 1 h, 2 h, 6 h, 24 h, 30 h, 36 h, 48 h, 72 h, and 96 h, animals were anesthetized with a mixture of ketamine (80 mg/kg) and xylazine (15 mg/kg) and blood was collected by heart puncture. The Au concentration in blood serum was determined by graphite furnace atomic absorption spectroscopy, using the atomic absorption spectrometer AAnalyst 600/Autosampler AS800 (PerkinElmer), equipped with a Gold (Au) Lumina Hollow Cathode Lamp (PerkinElmer #N305-0107), and using UltraClean THGA graphite tubes with an integrated platform (PerkinElmer #B3140361). Argon (Air Products Brasil #256431) was used as purge gas. BALB/c-derived serum samples were diluted (1:100) in a mixture of 0.2% HNO_3 and 10% HCl (v/v). Fifteen microliters of the samples was automatically pipetted together with 5 μL of matrix modifier: 0.005 mg of paladium ($Pd(NO_3)_2$ in 15% HNO_3, PerkinElmer #BO190635) and 0.003 mg of magnesium ($Mg(NO_3)_2$, PerkinElmer #BO190634). Pyrolysis and atomization temperatures were previously adjusted for 1100 and 1900 °C, respectively. A furnace program was established as presented in Table S2. Briefly, two drying steps of 110−130 °C were performed with a ramp time of 1 and 15 s, respectively, and a 30 s hold time each followed by pyrolysis, atomization, and furnace cleaning (2400 °C). The reading step, during atomization, was defined as 3 s without gas flow. A standard curve was performed for each independent experiment, using the gold standard: 1000 μg/L Au in 10% HCl (PerkinElmer #N9303759) in the presence of mice serum (1:100) (Figure S4). A blank matrix (serum without Au) was read and set as the background signal. The method for Au determination by atomic absorption showed suitable levels of precision and linearity. The software WinLab32 for AA (PerkinElmer) was used to control the AAnalyst600 and data acquisition.

Pharmacokinetic parameters were determined using the Rstrip 4.03 software. Experimental mean Au concentration−time data were submitted to iterative weighted nonlinear least-squares regression, and model selection was guided by Akaike's information criterion (application of Akaike's information criterion (AIC) in the evaluation of linear pharmacokinetic equations).[92] Data was best fitted by a two-exponential model with oral bolus input. Fitted parameters included maximum serum concentration of Au (C_{max}), the time for reaching the peak of serum Au concentration (T_{max}), the mean residence time of Au projected to infinity (MRT), the area under the serum concentration−time curve projected to infinity (AUC),

https://dx.doi.org/10.1021/acsinfecdis.9b00505
ACS Infect. Dis. XXXX, XXX, XXX−XXX

the absorption and elimination phase half-life [$T_{1/2}$ (abs) and $T_{1/2}$ (el)].

Interaction with Bovine Serum Albumin (BSA). The well-known structure of 580 amino acid residues of albumin contains two tryptophans, Trp-134 and Trp-212, which possess intrinsic fluorescence. Trp is highly sensitive to its local environment, resulting in protein conformational changes or binding to substrates,[93] allowing for the detection of those changes fluorometrically. Bovine serum albumin was purchased from Sigma-Aldrich (#A9418). A 1 μM solution of BSA was prepared in Tris−HCl (pH 7.4). The concentration was confirmed using UV−vis spectroscopy ($\varepsilon_{280\ nm}$ = 43 824 M^{-1} cm^{-1}). Gold(I) compounds were dissolved in DMSO to achieve 10 mM stock solutions and diluted to 1 mM in Tris−HCl. Ten aliquots were added to 2.5 mL of BSA solution in a quartz cuvette with a 1 cm optical path to a final concentration range of 0−60 μM (<1% DMSO v/v). The fluorescence spectra were recorded on a Cary Eclipse fluorescence spectrometer (Varian). The samples were excited at 280 nm, and the emission spectra were recorded from 300 to 500 nm with the slit set to 4 nm. The samples were measured at 300 s following the addition of each gold(I) compound while stirring. To infer about the mode of interaction, the experiments were performed at three different temperatures 25, 30, and 35 °C. The equations used can be found in the Supporting Information; constants and thermodynamic data are presented in Table S3.

***In Vivo* Toxicology.** BALB/c mice treated with gold(I) complexes (from the efficacy assay) were anesthetized with a mixture of ketamine (80 mg/kg) and xylazine (15 mg/kg), and blood was collected by puncture of the brachial plexus. Blood was centrifuged (3000 rpm, 15 min), and the obtained serum was frozen at −70 °C. The tests were performed in the Bioplus BIO-2000 semiautomatic analyzer (São Paulo, Brazil) using commercial kits (Labtest, Lagoa Santa, Brazil). Renal function was evaluated by measuring urea and creatinine. Liver function was evaluated by measuring alanine aminotransferase (ALT) and aspartate aminotransferase (AST) activity.

■ ASSOCIATED CONTENT

Supporting Information

The Supporting Information is available free of charge at https://pubs.acs.org/doi/10.1021/acsinfecdis.9b00505.

Sensitivity profiles of *Leishmania infantum*, *Leishmania braziliensis*, and THP-1 macrophages to gold(I) complexes; correlation analysis; *in vitro* combination of gold(I) complexes AdO Et or AdT Et and miltefosine; furnace program used to measure gold traces; electron spectroscopic imaging; calibration curve for atomic absorption gold trace elemental analysis and the pharmacokinetic profile of mice orally treated with gold complexes; intracellular levels of Au in *Leishmania infantum* exposed to gold(I) complexes; values of the Stern−Volmer quenching constant, apparent binding constant, number of binding sites, and thermodynamic parameters; chemicals and synthesis of gold(I) complexes (PDF)

Accession Codes

1BZL: Crystal structure of *Trypanosoma cruzi* trypanothione reductase in complex with trypanothione; DOI: 10.2210/pdb1BZL/pdb. 2JK6: Structure of Trypanothione Reductase from Leishmania infantum; DOI: 10.2210/pdb2JK6/pdb. All structures are from previously published studies where atomic coordinates and experimental details can be found.

■ AUTHOR INFORMATION

Corresponding Author

Rubens L. do Monte-Neto − *Instituto René Rachou/Fiocruz Minas−Fundação Oswaldo Cruz, Belo Horizonte 30190-009, Brasil;* orcid.org/0000-0002-4688-2462; Phone: +55 31 9 7132-7928; Email: rubens.monte@fiocruz.br

Authors

Luiza G. Tunes − *Instituto René Rachou/Fiocruz Minas−Fundação Oswaldo Cruz, Belo Horizonte 30190-009, Brasil*

Roberta E. Morato − *Instituto René Rachou/Fiocruz Minas−Fundação Oswaldo Cruz, Belo Horizonte 30190-009, Brasil*

Adriana Garcia − *Departamento de Química, Instituto de Ciências Exatas, Universidade Federal de Juiz de Fora, Juiz de Fora 36036-900, Brasil*

Vinicius Schmitz − *Departamento de Química, Instituto de Ciências Exatas, Universidade Federal de Juiz de Fora, Juiz de Fora 36036-900, Brasil*

Mario Steindel − *Departamento de Microbiologia, Imunologia e Parasitologia, Universidade Federal de Santa Catarina, Florianópolis 88040-900, Brasil*

José D. Corrêa-Junior − *Departamento de Morfologia, Universidade Federal de Minas Gerais, Belo Horizonte 31270-901, Brasil*

Hélio F. Dos Santos − *Departamento de Química, Instituto de Ciências Exatas, Universidade Federal de Juiz de Fora, Juiz de Fora 36036-900, Brasil;* orcid.org/0000-0003-0196-2642

Frédéric Frézard − *Departamento de Fisiologia e Biofísica, Universidade Federal de Minas Gerais, Belo Horizonte 31270-901, Brasil*

Mauro V. de Almeida − *Departamento de Química, Instituto de Ciências Exatas, Universidade Federal de Juiz de Fora, Juiz de Fora 36036-900, Brasil*

Heveline Silva − *Departamento de Química, Universidade Federal de Minas Gerais, Belo Horizonte 31270-901, Brasil;* orcid.org/0000-0003-3537-4961

Nilmar S. Moretti − *Departamento de Microbiologia, Imunologia e Parasitologia, Universidade Federal de São Paulo, São Paulo 04023-062, Brasil*

André L. B. de Barros − *Faculdade de Farmácia, Universidade Federal de Minas Gerais, Belo Horizonte 31270-901, Brasil*

Complete contact information is available at: https://pubs.acs.org/10.1021/acsinfecdis.9b00505

Author Contributions

Conceptualization and experimental design: L.G.T. and R.L.M.-N. Investigation/performed experiments: L.G.T., R.E.M., H.S., A.L.B.B., N.S.M., V.S., H.F.S., and R.L.M.-N. Synthesized the compounds: A.G., H.S., and M.V.A. Analyzed the data: L.G.T., R.E.M., F.F., H.S., M.S., A.L.B.B., N.S.M., and R.L.M.-N. Contributed to reagents/materials/analysis/tools: F.F., A.G., M.S., M.V.A., H.S., A.L.B.B., N.S.M., and R.L.M.-N. Supervision: R.L.M.-N. Writing, original draft: L.G.T. and R.L.M.-N. Writing, review and editing: L.G.T., R.L.M.-N., H.S., N.S.M., F.F., M.S., M.V.A., and A.L.B.B.

Notes

The authors declare no competing financial interest.

https://dx.doi.org/10.1021/acsinfecdis.9b00505
ACS Infect. Dis. XXXX, XXX, XXX−XXX

■ ACKNOWLEDGMENTS

The authors thank Dr. Silvia Reni Bortolin Uliana, Universidade de São Paulo, for providing the *L. braziliensis* H3227 LUC strain; Dr. Rodrigo Soares, Instituto René Rachou − Fiocruz Minas, Belo Horizonte, for his suggestions and for kindly providing the *L. amazonensis* PH8 LUC strain; Dr. Pedro Costa and Dr. Ricardo Gazzinelli, Instituto René Rachou − Fiocruz Minas, Belo Horizonte, who trained Luiza Tunes on the SeaHorse assays and allowed us to use the SeaHorse/Agilent XFe96 analyzer; Dr. Milene Hoehr de Moraes, Department of Microbiology, Immunology and Parasitology, Universidade Federal de Santa Catarina, Florianópolis, for technical assistance with the TR inhibition assay; MSc Juliana de Oliveira Silva, Pharmacy School, Universidade Federal de Minas Gerais for technical support with the toxicology assays. We also thank Brian Dockter for his constructive criticism and diligent proofreading of this manuscript. H.F.S. thanks Fapemig-CEX-APQ-00591-15 for supporting the NEQC laboratory. This work was financed in part by the Coordenação de Aperfeiçoamento de Pessoal de Nível Superior − Brasil (Capes) with an award to L.G.T. for a Ph.D. (Proap-Capes) scholarship. This work was funded by Fundação de Amparo à Pesquisa do Estado de Minas Gerais − Fapemig (grant number #APQ-03059-16) and by the International Society for Infectious Diseases (ISID Research Grant) to R.L.M.-N. N.S.M. is supported by Fundação de Amparo à Pesquisa do Estado de São Paulo − Fapesp (2018/09948-0). F.F. and R.L.M.-N. are CNPq Research Fellows (#305659/2017-0; #310640/2017-2). R.L.M.-N. is a grantee of Instituto Serrapilheira (grant number #3660). The funders had no role in the study design, data collection and analysis, decision to publish, or preparation of the manuscript.

■ ABBREVIATIONS

TR, trypanothione reductase (TSHR, reduced form or TcTR, *Trypanosoma cruzi*-derived TR); Au(PEt3)Cl, chloro(triethylphosphine)gold(I); Au(PPh3)Cl, chloro(triphenylphosphine)gold(I); ROS, reactive oxygen species; SbR, antimony-resistant *Leishmania* parasites; DTNB, 5,5′-dithiobis(2-nitrobenzoic acid); TNB, 2-nitro-5-thiobenzoate anion; MTT, 3-(4,5-dimethyl-2-thiazolyl)-2,5-diphenyl-2*H*-tetrazolium bromide; H_2-DCFDA, 2′,7′-dichlorodihydrofluorescein diacetate; HEPES, 4-(2-hydroxyethyl)piperazine-1-ethanesulfonic acid; OCR, oxygen consumption rate; ECAR, extracellular acidification rate; SbR, antiomony-resistant strain; EDX, energy-dispersive X-ray; FIC, fractional inhibitory concentration; DMSO, dimethylsufoxide

■ REFERENCES

(1) World Health Organization. (2015) *Investing to Overcome the Global Impact of Neglected Tropical Diseases: Third WHO Report on Neglected Diseases*, WHO Press.

(2) Amato, V. S., Tuon, F. F., Bacha, H. A., Neto, V. A., and Nicodemo, A. C. (2008) Mucosal Leishmaniasis. Current Scenario and Prospects for Treatment. *Acta Trop. 105*, 1−9.

(3) Silveira, F. T., Lainson, R., De Castro Gomes, C. M., Laurenti, M. D., and Corbett, C. E. P. (2009) Immunopathogenic Competences of *Leishmania (V.) braziliensis* and *L. (L.) amazonensis* in American Cutaneous Leishmaniasis. *Parasite Immunol. 31*, 423−431.

(4) Uliana, S. R. B., Trinconi, C. T., and Coelho, A. C. (2018) Chemotherapy of Leishmaniasis: Present Challenges. *Parasitology 145*, 464−480.

(5) Taslimi, Y., Zahedifard, F., and Rafati, S. (2018) Leishmaniasis and Various Immunotherapeutic Approaches. *Parasitology 145*, 497−507.

(6) Da Silva Maia, P. I., Deflon, V. M., and Abram, U. (2014) Gold(III) Complexes in Medicinal Chemistry. *Future Med. Chem. 6*, 1515−1536.

(7) Bertrand, B., and Casini, A. (2014) A Golden Future in Medicinal Inorganic Chemistry: The Promise of Anticancer Gold Organometallic Compounds. *Dalt. Trans. 43*, 4209−4219.

(8) Mora, M., Gimeno, M. C., and Visbal, R. (2019) Recent Advances in Gold-NHC Complexes with Biological Properties. *Chem. Soc. Rev. 48*, 447.

(9) Elie, B. T., Fernández-Gallardo, J., Curado, N., Cornejo, M. A., Ramos, J. W., and Contel, M. (2019) Bimetallic Titanocene-Gold Phosphane Complexes Inhibit Invasion, Metastasis, and Angiogenesis-Associated Signaling Molecules in Renal Cancer. *Eur. J. Med. Chem. 161*, 310−322.

(10) Curado, N., Dewaele-Le Roi, G., Poty, S., Lewis, J. S., and Contel, M. (2019) Trastuzumab Gold-Conjugates: Synthetic Approach and *in vitro* Evaluation of Anticancer Activities in Breast Cancer Cell Lines. *Chem. Commun. (Cambridge, U. K.) 55*, 1394.

(11) Carboni, S., Zucca, A., Stoccoro, S., Maiore, L., Arca, M., Ortu, F., Artner, C., Keppler, B. K., Meier-Menches, S. M., Casini, A., and Cinellu, M. (2018) New Variations on the Theme of Gold(III) C ^ N ^ N Cyclometalated Complexes as Anticancer Agents: Synthesis and Biological Characterization. *Inorg. Chem. 57*, 14852−14865.

(12) Li, X., Huang, Q., Long, H., Zhang, P., Su, H., and Liu, J. (2019) A New Gold(I) Complex-Au(PPh3)PT Is a Deubiquitinase Inhibitor and Inhibits Tumor Growth. *EBioMedicine 39*, 159.

(13) Nobili, S., Mini, E., Landini, I., et al. (2010) Gold Compounds as Anticancer Agents: Chemistry, Cellular Pharmacology, and Preclinical Studies. *Med. Res. Rev. 30*, 550−580.

(14) Paloque, L., Hemmert, C., Valentin, A., and Gornitzka, H. (2015) Synthesis, Characterization, and Antileishmanial Activities of Gold(I) Complexes Involving Quinoline Functionalized N -Heterocyclic Carbenes. *Eur. J. Med. Chem. 94*, 22−29.

(15) Zhang, C., Bourgeade Delmas, S., Fernández Álvarez, Á., Valentin, A., Hemmert, C., and Gornitzka, H. (2018) Synthesis, Characterization, and Antileishmanial Activity of Neutral N-Heterocyclic Carbenes Gold(I) Complexes. *Eur. J. Med. Chem. 143*, 1635−1643.

(16) Vieites, M., Smircich, P., Guggeri, L., Marchán, E., Gómez-Barrio, A., Navarro, M., Garat, B., and Gambino, D. (2009) Synthesis and Characterization of a Pyridine-2-Thiol N-Oxide Gold(I) Complex with Potent Antiproliferative Effect against *Trypanosoma cruzi* and *Leishmania* sp. Insight into Its Mechanism of Action. *J. Inorg. Biochem. 103*, 1300−1306.

(17) Navarro, M., Hernández, C., Colmenares, I., Hernández, P., Fernández, M., Sierraalta, A., and Marchán, E. (2007) Synthesis and Characterization of [Au(Dppz)2]Cl3. DNA Interaction Studies and Biological Activity against *Leishmania (L) mexicana*. *J. Inorg. Biochem. 101*, 111−116.

(18) Massai, L., Messori, L., Micale, N., Schirmeister, T., Maes, L., Fregona, D., Cinellu, M. A., and Gabbiani, C. (2017) Gold Compounds as Cysteine Protease Inhibitors: Perspectives for Pharmaceutical Application as Antiparasitic Agents. *BioMetals 30*, 313−320.

(19) Chaves, J. D. S., Tunes, L. G., J. Franco, C. H. J., Francisco, T. M., Corrêa, C. C., Murta, S. M. F., Monte-Neto, R. L., Silva, H., Fontes, A. P. S., and de Almeida, M. V. (2017) Novel Gold(I) Complexes with 5-Phenyl-1,3,4-Oxadiazole-2-Thione and Phosphine as Potential Anticancer and Antileishmanial Agents. *Eur. J. Med. Chem. 127*, 727−739.

(20) Angelucci, F., Sayed, A. A., Williams, D. L., Boumis, G., Brunori, M., Dimastrogiovanni, D., Miele, A. E., Pauly, F., and Bellelli, A. (2009) Inhibition of *Schistosoma mansoni* Thioredoxin-Glutathione Reductase by Auranofin. Structural and Kinetic Aspects. *J. Biol. Chem. 284*, 28977−28985.

https://dx.doi.org/10.1021/acsinfecdis.9b00505
ACS Infect. Dis. XXXX, XXX, XXX−XXX

(21) Bulman, C. a, Bidlow, C. M., Lustigman, S., Cho-Ngwa, F., Williams, D., Rascón, A. A., Jr., Tricoche, N., Samje, M., Bell, A., Suzuki, B., Lim, K., Supakorndej, N., Supakorndej, P., Wolfe, A., Knudsen, G., Chen, S., Wilson, C., Ang, K., Arkin, M., Gut, J., Franklin, C., Marcellino, C., McKerrow, J., Debnath, A., and Sakanari, J. (2015) Repurposing Auranofin as a Lead Candidate for Treatment of Lymphatic Filariasis and Onchocerciasis. *PLoS Neglected Trop. Dis. 9*, e0003534.

(22) Martínez-González, J. J., Guevara-Flores, A., Rendón, J. L., and Arenal, I. P. D. (2015) Auranofin-Induced Oxidative Stress Causes Redistribution of the Glutathione Pool in *Taenia crassiceps* Cysticerci. *Mol. Biochem. Parasitol. 201*, 16−25.

(23) Sannella, A. R., Casini, A., Gabbiani, C., Messori, L., Bilia, A. R., Vincieri, F. F., Majori, G., and Severini, C. (2008) New Uses for Old Drugs. Auranofin, a Clinically Established Antiarthritic Metallodrug, Exhibits Potent Antimalarial Effects *in vitro*: Mechanistic and Pharmacological Implications. *FEBS Lett. 582*, 844−847.

(24) Peroutka-Bigus, N., and Bellaire, B. H. (2019) Antiparasitic Activity of Auranofin against Pathogenic *Naegleria Fowleri*. *J. Eukaryotic Microbiol. 66*, 684.

(25) Lee, D., Xu, I. M.-J., Chiu, D. K.-C., Leibold, J., Tse, A. P.-W., Bao, M. H.-R., Yuen, V. W.-H., Chan, C. Y.-K., Lai, R. K.-H., Chin, D. W.-C., Chan, D., Cheung, T., Chok, S.-H, Wong, C.-M, Lowe, S., Ng, I. O.-L., and Wong, C. C.-L. (2019) Induction of Oxidative Stress via Inhibition of Thioredoxin Reductase 1 Is an Effective Therapeutic Approach for Hepatocellular Carcinoma. *Hepatology 69*, 1768.

(26) Sharlow, E. R., Leimgruber, S., Murray, S., Lira, A., Sciotti, R. J., Hickman, M., Hudson, T., Leed, S., Caridha, D., Barrios, A. M., Close, D., Grögl, M., and Lazo, J. (2014) Auranofin Is an Apoptosis-Simulating Agent with *in vitro* and *in vivo* Anti-Leishmanial Activity. *ACS Chem. Biol. 9*, 663−672.

(27) Ilari, A., Baiocco, P., Messori, L., Fiorillo, A., Boffi, A., Gramiccia, M., Di Muccio, T., and Colotti, G. (2012) A Gold-Containing Drug against Parasitic Polyamine Metabolism: The X-Ray Structure of Trypanothione Reductase from *Leishmania infantum* in Complex with Auranofin Reveals a Dual Mechanism of Enzyme Inhibition. *Amino Acids 42*, 803−811.

(28) Garcia, A., Machado, R. C., Grazul, R. M., Lopes, M. T. P., Corrêa, C. C., Dos Santos, H. F., de Almeida, M. V., and Silva, H. (2016) Novel Antitumor Adamantane-Azole Gold(I) Complexes as Potential Inhibitors of Thioredoxin Reductase. *JBIC, J. Biol. Inorg. Chem. 21*, 275−292.

(29) Colotti, G., Ilari, A., Fiorillo, A., Baiocco, P., Cinellu, M. A., Maiore, L., Scaletti, F., Gabbiani, C., and Messori, L. (2013) Metal-Based Compounds as Prospective Antileishmanial Agents: Inhibition of Trypanothione Reductase by Selected Gold Complexes. *ChemMedChem 8*, 1634−1637.

(30) Saravanamuthu, A., Vickers, T. J., Bond, C. S., Peterson, M. R., Hunter, W. N., and Fairlamb, A. H. (2004) Two Interacting Binding Sites for Quinacrine Derivatives in the Active Site of Trypanothione Reductase. *J. Biol. Chem. 279*, 29493−29500.

(31) Baiocco, P., Colotti, G., Franceschini, S., and Ilari, A. (2009) Molecular Basis of Antimony Treatment in Leishmaniasis. *J. Med. Chem. 52*, 2603−2612.

(32) Wyllie, S., Cunningham, M. L., and Fairlamb, A. H. (2004) Dual Action of Antimonial Drugs on Thiol Redox Metabolism in the Human Pathogen *Leishmania donovani*. *J. Biol. Chem. 279*, 39925−39932.

(33) Odds, F. C. (2003) Synergy, Antagonism, and What the Chequerboard Puts between Them. *J. Antimicrob. Chemother. 52*, 1.

(34) Oliveira, G. (2014) Cancer and Parasitic Infections: Similarities and Opportunities for the Development of New Control Tools. *Rev. Soc. Bras. Med. Trop. 47*, 1−2.

(35) Foscolos, A.-S., Papanastasiou, I., Tsotinis, A., Kolocouris, N., Foscolos, G. B., Vocat, A., and Cole, S. T. (2017) Synthesis of Adamantane Aminoethers with Antitubercular Potential. *Med. Chem. (Sharjah, United Arab Emirates) 13*, 670−681.

(36) Ilari, A., Fiorillo, A., Genovese, I., and Colotti, G. (2017) An Update on Structural Insights into the Enzymes of the Polyamine-Trypanothione Pathway: Targets for New Drugs against Leishmaniasis. *Future Med. Chem. 9*, 61−77.

(37) Cunningham, M. L., and Fairlamb, A. H. (1995) Trypanothione Reductase from *Leishmania donovani*. Purification, Characterisation and Inhibition by Trivalent Antimonials. *Eur. J. Biochem. 230*, 460−468.

(38) Turcano, L., Torrente, E., Missineo, A., Andreini, M., Gramiccia, M., Di Muccio, T., Genovese, I., Fiorillo, A., Harper, S., Bresciani, A., Colotti, G., and Ilari, A. (2018) Identification and Binding Mode of a Novel *Leishmania* Trypanothione Reductase Inhibitor from High Throughput Screening. *PLoS Neglected Trop. Dis. 12*, No. e0006969.

(39) Beig, M., Oellien, F., Garoff, L., Noack, S., Krauth-Siegel, R. L., and Selzer, P. M. (2015) Trypanothione Reductase: A Target Protein for a Combined *In vitro* and *In silico* Screening Approach. *PLoS Neglected Trop. Dis. 9*, No. e0003773.

(40) Krieger, S., Schwarz, W., Ariyanayagam, M. R., Fairlamb, A. H., Krauth-Siegel, R. L., and Clayton, C. (2000) Trypanosomes Lacking Trypanothione Reductase Are Avirulent and Show Increased Sensitivity to Oxidative Stress. *Mol. Microbiol. 35*, 542−552.

(41) Tovar, J., Wilkinson, S., Mottram, J. C., and Fairlamb, A. H. (1998) Evidence That Trypanothione Reductase Is an Essential Enzyme in *Leishmania* by Targeted Replacement of the TryA Gene Locus. *Mol. Microbiol. 29*, 653−660.

(42) Tovar, J. (1996) Extrachromosomal, Homologous Expression of Trypanothione Reductase and Its Complementary MRNA in *Trypanosoma cruzi*. *Nucleic Acids Res. 24*, 2942−2949.

(43) Altaf, M., Monim-Ul-Mehboob, M., Kawde, A.-N., Corona, G., Larcher, R., Ogasawara, M., Casagrande, N., Celegato, M., Borghese, C., Siddik, Z. H., Aldinucci, D., and Isab, A. A. (2017) New Bipyridine Gold(III) Dithiocarbamate-Containing Complexes Exerted a Potent Anticancer Activity against Cisplatin-Resistant Cancer Cells Independent of P53 Status. *Oncotarget 8*, 490−505.

(44) Gandin, V., Fernandes, A. P., Rigobello, M. P., Dani, B., Sorrentino, F., Tisato, F., Björnstedt, M., Bindoli, A., Sturaro, A., Rella, R., and Marzano, C. (2010) Cancer Cell Death Induced by Phosphine Gold(I) Compounds Targeting Thioredoxin Reductase. *Biochem. Pharmacol. 79*, 90−101.

(45) Al-Mohammed, H. I., Chance, M. L., and Bates, P. A. (2005) Production and Characterization of Stable Amphotericin-Resistant Amastigotes and Promastigotes of *Leishmania mexicana*. *Antimicrob. Agents Chemother. 49*, 3274−3280.

(46) Natera, S., Machuca, C., Padrón-Nieves, M., Romero, A., Díaz, E., and Ponte-Sucre, A. (2007) *Leishmania* spp.: Proficiency of Drug-Resistant Parasites. *Int. J. Antimicrob. Agents 29*, 637−642.

(47) Hendrickx, S., Leemans, A., Mondelaers, A., Rijal, S., Khanal, B., Dujardin, J. C., Delputte, P., Cos, P., and Maes, L. (2015) Comparative Fitness of a Parent *Leishmania donovani* Clinical Isolate and Its Experimentally Derived Paromomycin-Resistant Strain. *PLoS One 10*, e0140139.

(48) Rush, G. F., Smith, P. F., Alberts, D. W., Mirabelli, C. K., Snyder, R. M., Crooke, S. T., Sowinski, J., Jones, H. B., and Bugelski, P. J. (1987) The Mechanism of Acute Cytotoxicity of Triethylphosphine Gold(I) Complexes. I. Characterization of Triethylphosphine Gold Chloride-Induced Biochemical and Morphological Changes in Isolated Hepatocytes. *Toxicol. Appl. Pharmacol. 90*, 377−390.

(49) de Souza Queiroz, D. P., Carollo, C. A., Toffoli Kadri, M. C., Rizk, Y. S., de Araujo, V. C. P., de Oliveira Monteiro, P. E., Rodrigues, P. O., Oshiro, E. T., Matos, M. D. F. C., and de Arruda, C. C. P. (2016) *In vivo* Antileishmanial Activity and Chemical Profile of Polar Extract from *Selaginella sellowii*. *Mem. Inst. Oswaldo Cruz 111*, 147−154.

(50) Gopinath, V. S., Pinjari, J., Dere, R. T., Verma, A., Vishwakarma, P., Shivahare, R., Moger, M., Kumar Goud, P. S., Ramanathan, V., Bose, P., Rao, M. V. S., Gupta, S., Puri, S. K., Launay, D., and Martin, D. (2013) Design, Synthesis and Biological Evaluation of 2-Substituted Quinolines as Potential Antileishmanial Agents. *Eur. J. Med. Chem. 69*, 527−536.

https://dx.doi.org/10.1021/acsinfecdis.9b00505
ACS Infect. Dis. XXXX, XXX, XXX−XXX

(51) Gupta, S., Tiwari, S., Bhaduri, A. P., and Jain, G. K. (2002) Anilino-(2-Bromophenyl) Acetonitrile: A Promising Orally Effective Antileishmanial Agent. *Acta Trop. 84*, 165−173.
(52) Isakov, E., Weisman-Shomer, P., and Benhar, M. (2014) Suppression of the Pro-Inflammatory NLRP3/Interleukin-1β Pathway in Macrophages by the Thioredoxin Reductase Inhibitor Auranofin. *Biochim. Biophys. Acta, Gen. Subj. 1840*, 3153−3161.
(53) Křikavová, R., Hošek, J., Suchý, P., Vančo, J., and Trávníček, Z. (2014) Diverse *in vitro* and *in vivo* Anti-Inflammatory Effects of Trichlorido-Gold(III) Complexes with N6-Benzyladenine Derivatives. *J. Inorg. Biochem. 134*, 92−99.
(54) Trávníček, Z., Štarha, P., Vančo, J., Šilha, T., Hošek, J., Suchý, P., and Pražanová, G. (2012) Anti-Inflammatory Active Gold(I) Complexes Involving 6-Substituted-Purine Derivatives. *J. Med. Chem. 55*, 4568−4579.
(55) Trinconi, C. T., Reimão, J. Q., Coelho, A. C., and Uliana, S. R. B. (2016) Efficacy of Tamoxifen and Miltefosine Combined Therapy for Cutaneous Leishmaniasis in the Murine Model of Infection with *Leishmania amazonensis*. *J. Antimicrob. Chemother. 71*, 1314−1322.
(56) Sundar, S., Rai, M., Chakravarty, J., Agarwal, D., Agrawal, N., Vaillant, M., Olliaro, P., and Murray, H. W. (2008) New Treatment Approach in Indian Visceral Leishmaniasis: Single-Dose Liposomal Amphotericin B Followed by Short-Course Oral Miltefosine. *Clin. Infect. Dis. 47*, 1000−1006.
(57) Anand, D., Yadav, P. K., Patel, O. P. S., Parmar, N., Maurya, R. K., Vishwakarma, P., Raju, K. S. R., Taneja, I., Wahajuddin, M., Kar, S., and Yadav, P. P. (2017) Antileishmanial Activity of Pyrazolopyridine Derivatives and Their Potential as an Adjunct Therapy with Miltefosine. *J. Med. Chem. 60*, 1041−1059.
(58) Tiwari, B., Pahuja, R., Kumar, P., Rath, S. K., Gupta, K. C., and Goyal, N. (2017) Nanotized Curcumin and Miltefosine, a Potential Combination for the Treatment of Experimental Visceral Leishmaniasis. *Antimicrob. Agents Chemother. 61*, e01169-16.
(59) Neault, J. F., and Tajmir-Riahi, H. A. (1998) Interaction of Cisplatin with Human Serum Albumin. Drug Binding Mode and Protein Secondary Structure. *Biochim. Biophys. Acta, Protein Struct. Mol. Enzymol. 1384*, 153−159.
(60) García-Moreno, E., Tomás, A., Atrián-Blasco, E., Gascón, S., Romanos, E., Rodriguez-Yoldi, M. J., Cerrada, E., and Laguna, M. (2016) *In vitro* and *in vivo* Evaluation of Organometallic Gold(I) Derivatives as Anticancer Agents. *Dalt. Trans. 45*, 2462−2475.
(61) Gouvea, L. R., Garcia, L. S., Lachter, D. R., Nunes, P. R., de Castro Pereira, F., Silveira-Lacerda, E. P., Louro, S. R. W., Barbeira, P. J. S., and Teixeira, L. R. (2012) Atypical Fluoroquinolone Gold(III) Chelates as Potential Anticancer Agents: Relevance of DNA and Protein Interactions for Their Mechanism of Action. *Eur. J. Med. Chem. 55*, 67−73.
(62) Mandal, G., Bardhan, M., and Ganguly, T. (2010) Interaction of Bovine Serum Albumin and Albumin-Gold Nanoconjugates with l-Aspartic Acid. A Spectroscopic Approach. *Colloids Surf., B 81*, 178−184.
(63) Yue, H.-L., Hu, Y.-J., Chen, J., Bai, A.-M., and Ouyang, Y. (2014) Green Synthesis and Physical Characterization of Au Nanoparticles and Their Interaction with Bovine Serum Albumin. *Colloids Surf., B 122*, 107−114.
(64) Coffer, M. T., Shaw, C. F., Eidsness, M. K., Watkins, J. W., and Elder, R. C. (1986) Reactions of Auranofin and Chloro-(Triethylphosphine)Gold with Bovine Serum Albumin. *Inorg. Chem. 25*, 333−339.
(65) Ahmed, A., Al Tamimi, D. M., Isab, A. A., Alkhawajah, A. M. M., and Shawarby, M. A. (2012) Histological Changes in Kidney and Liver of Rats Due to Gold (III) Compound [Au(En)Cl2]Cl. *PLoS One 7*, e51889.
(66) Nair, A., and Jacob, S. (2016) A Simple Practice Guide for Dose Conversion between Animals and Human. *J. Basic Clin. Pharm. 7*, 27.
(67) Assis, T. S. M. de, Rosa, D. C. P., Teixeira, E. de M., Cota, G., Azeredo-Da-Silva, A. L. F., Werneck, G., and Rabello, A. (2017) The Direct Costs of Treating Human Visceral Leishmaniasis in Brazil. *Rev. Soc. Bras. Med. Trop. 50*, 478−482.
(68) de Carvalho, I. P. S. F., Peixoto, H. M., Romero, G. A. S., and de Oliveira, M. R. F. (2019) Treatment for Human Visceral Leishmaniasis: A Cost-Effectiveness Analysis for Brazil. *Trop. Med. Int. Health 24*, 1064.
(69) Sunyoto, T., Potet, J., and Boelaert, M. (2018) Why Miltefosine—a Life-Saving Drug for Leishmaniasis—Is Unavailable to People Who Need It the Most. *BMJ. Glob. Heal. 3*, No. e000709.
(70) Berger, B. A., Cossio, A., Saravia, N. G., Castro, M. d. M., Prada, S., Bartlett, A. H., and Pho, M. T. (2017) Cost-Effectiveness of Meglumine Antimoniate versus Miltefosine Caregiver DOT for the Treatment of Pediatric Cutaneous Leishmaniasis. *PLoS Neglected Trop. Dis. 11*, No. e0005459.
(71) Chaves, J. D. S., Neumann, F., Francisco, T. M., Corrêa, C. C., Lopes, M. T. P., Silva, H., Fontes, A. P. S., and De Almeida, M. V. (2014) Synthesis and Cytotoxic Activity of Gold(I) Complexes Containing Phosphines and 3-Benzyl-1,3-Thiazolidine-2-Thione or 5-Phenyl-1,3,4-Oxadiazole-2-Thione as Ligands. *Inorg. Chim. Acta 414*, 85−90.
(72) Coelho, A. C., Oliveira, J. C., Espada, C. R., Reimão, J. Q., Trinconi, C. T., and Uliana, S. R. B. (2016) A Luciferase-Expressing *Leishmania braziliensis* Line That Leads to Sustained Skin Lesions in BALB/c Mice and Allows Monitoring of Miltefosine Treatment Outcome. *PLoS Neglected Trop. Dis. 10*, e0004660.
(73) Rocha, M. N., Corrêa, C. M., Melo, M. N., Beverley, S. M., Martins-Filho, O. A., Madureira, A. P., and Soares, R. P. (2013) An Alternative in Vitro Drug Screening Test Using *Leishmania amazonensis* Transfected with Red Fluorescent Protein. *Diagn. Microbiol. Infect. Dis. 75*, 282−291.
(74) Habtemariam, S. (2003) *In vitro* Antileishmanial Effects of Antibacterial Diterpenes from Two Ethiopian Premna Species: *P. schimperi* and *P. oligotricha*. *BMC Pharmacol. 3*, 6.
(75) Ouellette, M., Fase-Fowler, F., and Borst, P. (1990) The Amplified H Circle of Methotrexate-Resistant *Leishmania tarentolae* Contains a Novel P-Glycoprotein Gene. *EMBO J. 9*, 1027−1033.
(76) Ouellette, M., Hettema, E., Wüst, D., Fase-Fowler, F., and Borst, P. (1991) Direct and Inverted DNA Repeats Associated with P-Glycoprotein Gene Amplification in Drug Resistant *Leishmania*. *EMBO J. 10*, 1009−1016.
(77) Roy, G., Dumas, C., Sereno, D., Wu, Y., Singh, A. K., Tremblay, M. J., Ouellette, M., Olivier, M., and Papadopoulou, B. (2000) Episomal and Stable Expression of the Luciferase Reporter Gene for Quantifying *Leishmania* spp. Infections in Macrophages and in Animal Models. *Mol. Biochem. Parasitol. 110*, 195−206.
(78) Mosmann, T. (1983) Rapid Colorimetric Assay for Cellular Growth and Survival: Application to Proliferation and Cytotoxicity Assays. *J. Immunol. Methods 65*, 55−63.
(79) Hamilton, C. J., Saravanamuthu, A., Eggleston, I. M., and Fairlamb, A. H. (2003) Ellman's-Reagent-Mediated Regeneration of Trypanothione *in situ*: Substrate-Economical Microplate and Time-Dependent Inhibition Assays for Trypanothione Reductase. *Biochem. J. 369*, 529−537.
(80) Bond, C. S., Zhang, Y., Berriman, M., Cunningham, M. L., Fairlamb, A. H., and Hunter, W. N. (1999) Crystal Structure of *Trypanosoma cruzi* Trypanothione Reductase in Complex with Trypanothione, and the Structure-Based Discovery of New Natural Product Inhibitors. *Structure 7*, 81−89.
(81) Baiocco, P., Poce, G., Alfonso, S., Cocozza, M., Porretta, G. C., Colotti, G., Biava, M., Moraca, F., Botta, M., Yardley, V., Fiorillo, A., Lantella, A., Malatesta, F., and Ilari, A. (2013) Inhibition of *Leishmania infantum* Trypanothione Reductase by Azole-Based Compounds: A Comparative Analysis with Its Physiological Substrate by x-Ray Crystallography. *ChemMedChem 8*, 1175−1183.
(82) Verdonk, M. L., Cole, J. C., Hartshorn, M. J., Murray, C. W., and Taylor, R. D. (2003) Improved Protein-Ligand Docking Using GOLD. *Proteins: Struct., Funct., Genet. 52*, 609−623.

https://dx.doi.org/10.1021/acsinfecdis.9b00505
ACS Infect. Dis. XXXX, XXX, XXX−XXX

(83) Korb, O., Stützle, T., and Exner, T. E. (2009) Empirical Scoring Functions for Advanced Protein-Ligand Docking with PLANTS. *J. Chem. Inf. Model. 49*, 84−96.
(84) Dos Santos, H. F. (2014) Reactivity of Auranofin with S-, Se- and N-Containing Amino Acids. *Comput. Theor. Chem. 1048*, 95−101.
(85) Baker, N. A., Sept, D., Joseph, S., Holst, M. J., and McCammon, J. A. (2001) Electrostatics of Nanosystems: Application to Microtubules and the Ribosome. *Proc. Natl. Acad. Sci. U. S. A. 98*, 10037−10041.
(86) Mukherjee, A., Boisvert, S., Monte-Neto, R. L., Coelho, A. C., Raymond, F., Mukhopadhyay, R., Corbeil, J., and Ouellette, M. (2013) Telomeric Gene Deletion and Intrachromosomal Amplification in Antimony-Resistant Leishmania. *Mol. Microbiol. 88*, 189−202.
(87) Shah-Simpson, S., Pereira, C. F. A., Dumoulin, P. C., Caradonna, K. L., and Burleigh, B. A. (2016) Bioenergetic Profiling of *Trypanosoma cruzi* Life Stages Using Seahorse Extracellular Flux Technology. *Mol. Biochem. Parasitol. 208*, 91−95.
(88) Ferrick, D. A., Neilson, A., and Beeson, C. (2008) Advances in Measuring Cellular Bioenergetics Using Extracellular Flux. *Drug Discovery Today 13*, 268−274.
(89) Furtado, C., Kunrath-Lima, M., Rajão, M. A., Mendes, I. C., de Moura, M. B., Campos, P. C., Macedo, A. M., Franco, G. R., Pena, S. D. J., Teixeira, S. M. R., Van Houten, B., and Machado, C. R. (2012) Functional Characterization of 8-Oxoguanine DNA Glycosylase of *Trypanosoma cruzi*. *PLoS One 7*, e42484.
(90) Trinconi, C. T., Reimão, J. Q., Yokoyama-Yasunaka, J. K. U., Miguel, D. C., and Uliana, S. R. B. (2014) Combination Therapy with Tamoxifen and Amphotericin B in Experimental Cutaneous Leishmaniasis. *Antimicrob. Agents Chemother. 58*, 2608−2613.
(91) Reimão, J. Q., Trinconi, C. T., Yokoyama-Yasunaka, J. K., Miguel, D. C., Kalil, S. P., and Uliana, S. R. B. (2013) Parasite Burden in *Leishmania (Leishmania) amazonensis*-Infected Mice: Validation of Luciferase as a Quantitative Tool. *J. Microbiol. Methods 93*, 95−101.
(92) Yamaoka, K., Nakagawa, T., and Uno, T. (1978) Application of Akaike's Information Criterion (AIC) in the Evaluation of Linear Pharmacokinetic Equations. *J. Pharmacokinet. Biopharm. 6*, 165−175.
(93) Ni, Y., Zhu, R., and Kokot, S. (2011) Competitive Binding of Small Molecules with Biopolymers: A Fluorescence Spectroscopy and Chemometrics Study of the Interaction of Aspirin and Ibuprofen with BSA. *Analyst 136*, 4794.

https://dx.doi.org/10.1021/acsinfecdis.9b00505
ACS Infect. Dis. XXXX, XXX, XXX−XXX